

AN-Najah National University

Facility of Graduated Studies

**Synthesis, Characterization, and CT-DNA Interactions
of Novel Complexes of (Copper(II)\ Tetradentate
SNNS Schiff Bases)**

By

Ibtihal Nedal Odeh

Supervisor

Prof. Ismail Warad

Co- Supervisor

Prof. Mohammed Al-Nuri

**This Thesis is Submitted in Partial Fulfillment of the Requirements for
the Degree of Master of Chemistry, Faculty of Graduate Studies, An-
Najah National University, Nablus, Palestine.**

2016

**Synthesis, Characterization, and CT-DNA Interactions
of Novel Complexes of (Copper(II)\ Tetradentate
SNNS Schiff Bases)**

**By
Ibtihal Nedal Odeh**

This thesis was defended successfully on 2/3/2016 and approved by:

Defense committee Members

Signature

– Prof. Ismail Warad /Supervisor

.....

– Prof. Mohammed Al-Nuri /Co-Supervisor

.....

– Dr. Sameer Amerieh /External Examiner

.....

– Dr. Mohammad Sulaiman /Internal Examiner

.....

III

Dedication

My Affectionate Parents

Brothers and Sisters.

Special Dedication To

My Father, Nedal

My husband, Waseem

With my Respect and Love

Acknowledgments

I would like to express my deep appreciation and respect to prof. Ismail warad(supervisor) and prof. Mohammed Al-Nuri (Co-supervisor) for their direct supervision, encouragement and help throughout the course of this work. Also, I would like to thank my committee members, Dr..... and Dr..... for their fruitful discussions.

Special thanks are due to my father, Nedal , my mother, Afaf , and my hasband, waseem , for their support and encouragement. Special thanks are presented to my brothers Osama , and Yousef. My sisters, Amal, Anwar ,Eman and Suha.

Thanks are also due to my friends , Particularly , RenadIssa , Baraa Omar, RemahAbd Al-Razeq.

Also , I would like to thank Mr. NafithDwikat for his support and laboratory helping and measurements.

Finally, thanks to Dr. Mohammad Sulaiman, Head of Department of Chemistry for his support and help, to Dr. Sameer Amerieh for his Suggestions.

الإقرار

أنا الموقع أدناه مقدم الرسالة التي تحمل العنوان

**Synthesis, Characterization, and CT-DNA Interactions of
Novel Complexes of (Copper(II)\ Tetradentate SNNS Schiff
Bases)**

أقر بأن ما شملت عليه الرسالة هو نتاج جهدي الخاص, باستثناء ما تمت الإشارة إليه حيثما ورد,
وأن هذه الرسالة ككل أو أي جزء منها لم يقدم من قبل لنيل أي درجة أو لقب علمي أو بحثي لدى
أي مؤسسة علمية أو بحثية

Declaration

The work provided in this thesis, unless otherwise referenced, is the researcher's own work, and has not been submitted elsewhere for any other degrees or qualifications.

Student's Name:

اسم الطالب: إتهال نضال محمود عودة

Signature

التوقيع: 

Date

2/3/2016

التاريخ:

List of Contents

No.	Contents	Page
	Dedication	III
	Acknowledgment	IV
	Declaration	V
	List of Contents	VI
	List of Figures	IX
	List of Tables	X
	List of Schemes	XI
	List of Charts	XII
	Abbreviations	XIII
	Abstract	XV
	Chapter 1: Introduction	1
1	The aim of this study	2
2	Definition and history of Schiff base	2
3	Chemical and physical properties	3
4	Importance and uses of Schiff base	3
4.1	Antibacterial activities	4
4.2	Antifungal activities	4
5	Coordination chemistry of Schiff base	4
5.1	Schiff bases as ligands and their uses	4
5.2	Why copper	5
6	Previous work	5
7	Green synthesis, spectral, thermal and X-ray single crystal analysis of 2-(5-bromothiophen-2-yl)-5,5-dimethylhexahydropyrimidine L_1 and their Cu(II) complexes 1-3	7
	Chapter 2: Experimental	9
1	Chemicals	10
2	Equipments	11
3	Synthesis	12
3.1	Synthesis of L_1	12
3.2	Synthesis of L_2	13
3.3	Synthesis of complex 1	13
3.4	Synthesis of complex 2	13
3.5	Synthesis of complex 3	13

3.6	Synthesis of complex 4	14
3.7	Synthesis of complex 5	14
3.8	Synthesis of complex 6	14
	Chapter 3: Result and Discussion	15
Part One	Green synthesis, spectral, thermal and X-ray single crystal analysis of 2-(5-bromothiophen-2-yl)-5,5-dimethylhexahydropyrimidine and their Cu(II) complexes	17
1	Single Crystal X-Ray Diffraction	17
2	Synthesis	19
2.1	Synthesis of L ₁	19
2.2	Synthesis of Complexes 1-3	19
3	EI-MS of L ₁	20
4	Frontier molecular orbital analysis of L ₁	21
5	UV-vis spectral analysis	22
6	FT-IR spectral analysis	25
6.1	FT-IR spectral analysis of L ₁	25
6.2	FT-IR spectral analysis of complexes 4-6	27
7	Thermal analysis investigation of L ₁	28
8	¹ H and ¹³ C NMR spectral analysis of L ₁	29
9	X-Ray structural determination investigation of L ₁	31
10	Hirshfeld surface analysis of L ₁	34
11	Conclusion	39
Part Two	Synthesis, spectral, and thermal Studies of N,N-Bis-thiophen-2-ylmethylene-cyclohexane-1,2-diamine and their Cu(II) complexes	42
1	Synthesis	42
1.1	Synthesis of L ₂	42
1.2	Synthesis of complexes 4-6	42
2	FT-IR- spectral analysis L ₂	43
2.1	FT-IR of L ₂ and starting materials	43
2.2	FT-IR of L ₂ and their complexes 4-6	45
3	NMR Spectral analysis of L ₂	48
3.1	¹ H NMR spectral analysis of L ₂	48
3.2	¹³ C NMR spectral analysis of L ₂	49
4	Cyclic Voltammetry of complex 5	49
5	Thermal analysis	51

VIII

5.1	Thermal analysis of L ₂	51
5.2	Thermal analysis of complex 4	52
6	Conclusion	53
7	Suggestions	55
	References	56
	الملخص	ب

List of Figures

No.	Figure	Page
1	TOF-MS spectrum of L ₁ .	21
2	HOMO and LUMO plots of L ₁	22
3	UV-Vis spectra of L ₁ in ethanol at room temperature a), TD-DFT/B3LYP/3-311++G UV-vis method b).	23
4	UV-Vis spectra of complexes 1 and 2 dissolved in EtOH at RT.	24
5	In situ Vis-spectra of a) free CuBr ₂ , b) CuL ₁ Br ₂ , c) CuL ₁ Cl ₂ , d) [Cu(L ₁) ₂ Br]Br and e) [Cu(L ₁) ₂ Cl]Cl dissolved in EtOH at RT.	25
6	IR spectra of: a) 2,2-dimethyl-1,3- propanediamine, b) 5-bromothiophen-2-carbaldehyde and c) L ₁ , d) calculated with B3LYP/3-311+G.	26
7	FT-IR spectrum of complex 1 and complex 2.	28
8	TG/DTG thermal curves of L ₁ a) and of the complex 1 b).	29
9	¹ H NMR spectrum of L ₁ dissolved in CDCl ₃ at RT.	30
10	¹³ C NMR spectrum of L ₁ dissolved in CDCl ₃ at RT.	30
11	ORTEP diagram of L ₁ with thermal ellipsoids drawn at 50% probability.	32
12	Packing of the L ₁ molecules when viewed down along the c-axis indicating layered stacking.	33
13	Fingerprint plots of L ₁ .	37
14	d _{norm} and electrostatic potential mapped on Hirshfeld surface for visualizing the intermolecular contacts. The ball and stick models represent the different orientations corresponding to the Hirshfeld surface and the electrostatic potential.	38
15	IR spectrum for a) Cyclohexane-1,2-diamine, b) Thiophene-2-carbaldehyde, c) L ₂	44
16	IR spectrum for a) Complex 4, b)Complex 5 ,c) Complex 6.	46
17	¹ H NMR spectrum of L ₂ dissolved in CDCl ₃ at RT	48
18	¹³ C NMR spectrum of L ₂ dissolved in CDCl ₃ at RT	49
19	Cyclic voltammogram of complex 5 in DMF solution, at scan rate 0.1 V/s	50
20	TG/DTG thermal curve of L ₂	51
21	TG/ DTG thermal curve of complex 4	53

List of Tables

No.	Table	Page
1	Crystal data and structure refinement details.	18
2	Bond lengths (Å).	34
3	Bond angles (°).	34

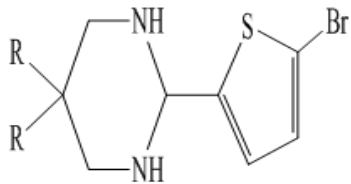
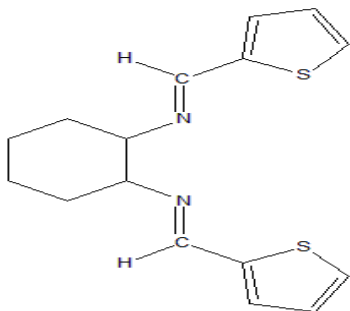
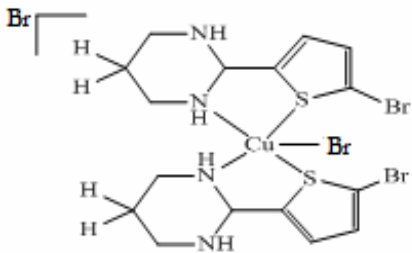
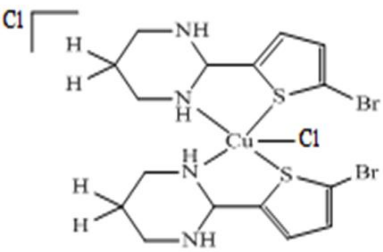
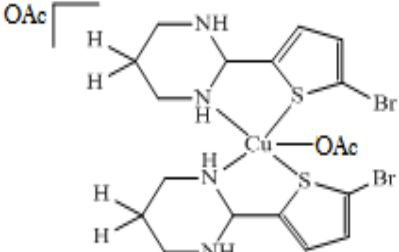
List of Schemes

No.	Scheme	Page
1	Synthesis of Schiff base	2
2	Reaction of thiophene-2-carbaldehyde with 2-aminoaniline.	6
3	Synthesis of L ₁ and their complexes 1-3	20
4	Synthesis of L ₂ and their complexes 4-6	43

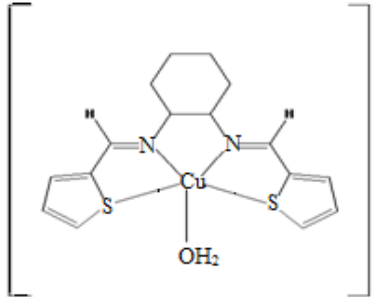
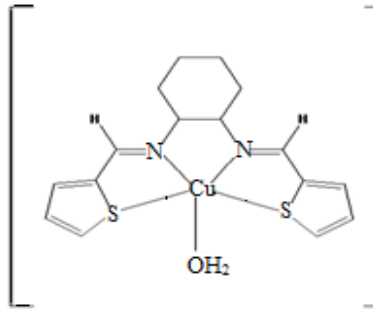
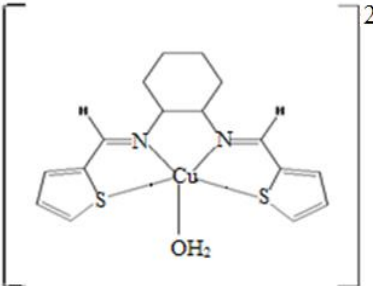
List of Charts

No.	Chart	page
1	N,N-bis-thiophen-2-ylmethylene-cyclohexane-1,4-diamine	6
2	N,N-bis-thiophen-2-ylm ethylene-propane-1,3-diamine	6
3	Expected structure of complex 1	39
4	Expected structure of complex 2	40
5	Expected structure of complex 3	40
6	Monocation and dicationic complexes	47
8	Expected structure of complex 4	54
9	Expected structure of complex 5	54
10	Expected structure of complex 6	54

Abbreviations

Symbol	Structure/ Name
L ₁	2-(5-bromothiophen-2-yl)-5,5 dimethylhexahydropyrimidine 
L ₂	N,N-bis-thiophen-2-ylmethylene-cyclohexane-1,2-diamine 
Complex 1	
Complex 2	
Complex 3	

XIV

Complex 4	 $\left[\text{Cu}(\text{OH}_2)(\text{L})_2 \right] 2\text{Br}^-$
Complex 5	 $\left[\text{Cu}(\text{OH}_2)(\text{L})_2 \right] 2\text{Cl}^-$
Complex 6	 $\left[\text{Cu}(\text{OH}_2)(\text{L})_2 \right] 2\text{OAc}^-$

**Synthesis, Characterization, and CT-DNA Interactions of Novel
Complexes of (Copper(II)\ Tetradentate SNNS Schiff Bases)**

By

Ibtihal Nedal Odeh

Supervisor

Prof. Ismail Warad

Co- Supervisor

Prof. Mohammed Al-Nuri

Abstract

This research focuses on synthesis of novel N-donor ligand, which are expected to be excellent chelator in coordination chemistry and synthesis of their complexes.

In part one, novel heterocyclic compound L_1 was synthesized by solvent-free condensation reaction of 5-bromothiophene-2-carbaldehyde with 2,2-dimethyl-1,3-propanediamine at mild condition. The desired product was characterized by FT-IR spectroscopy, X-ray single crystal diffraction, elemental analysis, TG\DTG, UV-visible spectroscopy, and ^1H NMR spectroscopy.

The binding ability of the new L_1 was evaluated using CuX_2 salt, $\text{X} = \text{Br}, \text{Cl}, \text{OAc}$, to form complex 1,2 and 3

Penta coordination around Cu(II) centers was characterized using FT- IR spectroscopy and TG/DTG analysis.

In part two, novel Schiff base; L_2 was also synthesized directly by mixing of thiophene-2-carbaldehyde with cyclohexane-1,2-diamine in ultrasonic path. The desired product was characterized by FT-IR spectroscopy, ^{13}C -NMR ^1H NMR spectroscopy, cyclic voltammetry, thermal analysis.

XVI

The desired Schiff base was used as tetradentate (N_2S_2) chelate ligand when coordinate with CuX_2 .

The $Cu(II)$ complexes 4, 5 and 6 formed by mixing 1:1 Schiff base with $Cu(II)$ was confirmed spectrally to be square pyramide dicationic complexes with one H_2O .

Chapter One

Introduction

Chapter One

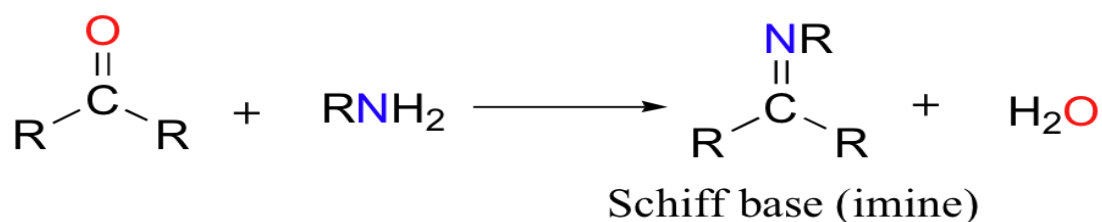
Introduction

1. The aims of this study are:

- ❖ To synthesize and characterize new Schiff base containing N₂S₂ donating atoms.
- ❖ To synthesize and characterize Schiff base Cu(II) complexes.
- ❖ To synthesize and characterize new dimethylhexahydropyrimidine compound, which is also considered to be excellent donating ligand.
- ❖ To synthesize and characterize heterocyclic Cu(II) complexes.

2. Definition and history of Schiff base

Schiff bases are an important class of organic compounds, they are produced from condensation reaction of primary amines and carbonyl compounds (Ketone or aldehyde) [1] as in **Scheme 1**.



Scheme 1: Synthesis of Schiff base

Schiff base was discovered by Hugo Schiff in 1964, he discovered several methods for their synthesis . Nowadays, many new methods have been published, such as, microwave radiation, clay, solvent-free, and molecular sieves[3].

3. Chemical and physical properties

Schiff bases have the structure of $\text{RHC}=\text{N-R1}$ where R and R1 are aryl; derived from aromatic ring, alkyl, heterocyclic groups, or cycloalkyl, they are also known as imine or azomethine in which carbonyl group $\text{C}=\text{O}$ of aldehyde or ketone is replaced by an imine or azomethine group $\text{C}=\text{N}$. The presence of a lone pair of electrons in sp^2 hybridized orbital of nitrogen atom ($\text{C}=\text{N}$) of Schiff bases gives them biological and chemical importance [1,6]. The spectral analysis (IR, NMR, XRD, UV-visible spectroscopy), and TG have been used to characterize and determine physical – chemical properties of Schiff bases [6].

4. Importance and uses of Schiff base

Several studies showed that the presence of a lone pair of electrons on nitrogen atom of imine group give it an incredible chemical and physical importance [6]. Because of their easy of synthesis, flexibility, and the special properties of $\text{C}=\text{N}$ Schiff bases are considered to be excellent donating ligand [7].

Schiff bases have been reported to exhibit a lot of biological activities that involve, antifungal, antitumor, antibacterial, herbicidal activities, anti-inflammatory, anti-malarial, antipyretic properties, and clinical, physiological, pharmacological, and anti HIV activities [1, 5-7,11-12]. Chemically, Schiff base complexes play an important role as a catalyst in medicine and in wide range of organic reactions e.g. epoxidation of olefin, trimethylsilyl-cyanation of ketones, ring opening polymerization of lactide.

In addition, Schiff base can be used as anti corrosion and in many organic synthesis as in [2-3,7].

In addition of biological and chemical uses, Schiff base plays an important role in deferent fields, such, dye industries, agriculture, plastic, physiology and providing liquid crystal [17].

4.1. Antibacterial activities

Because of the free radical scavenging ability of their metal complexes, Schiff bases showed a lot of antibacterial activities against various types of bacteria such *Salmonella typhi*, *Klebsiella pneumonia*, *Escherichia coli*, *pseudomonas* [13].

4.2. Antifungal activities

Schiff base polydentate ligands and their Copper(II) complexes showed excellent antifungal activities against various types of fungi such, *Rhizopusstolonifer*, *Rhizoctoniabataticola*, *Candida albicans*, *Aspergillus niger*, and *Aspergillus flavus* [12].

5. Coordination chemistry

5.1. Schiff bases as ligands and their uses

Schiff bases have been used as ligands in coordination chemistry because they have shown excellent sensitivity, selectivity and stability for specific metals such; Co(II), Ag(I), Gd(II), Cu(II), Ni(II), Hg(II), Y(III), Pd(II), Sn(II) and Zn(II), they have been used as cation carriers in potentiometric sensors. Their complexes have a great interest for many years, due to

diversity and structural variability, specially Schiff bases that containing N and S atoms which are considered to be an excellent donating atoms [4,8,11,14].

5.2. Why Copper ?

Copper, a bio-essential element, plays an important role in biological processes that involve electron transfer reactions, in fact copper(II) complexes with O, N, S have been widely studied and they are proved to be good anticancer agents due to their strong binding affinity with DNA [13-15]. It has been demonstrated that copper assembles in tumors due to the selective permeability of cancer cell membranes to copper compounds [13, 14].

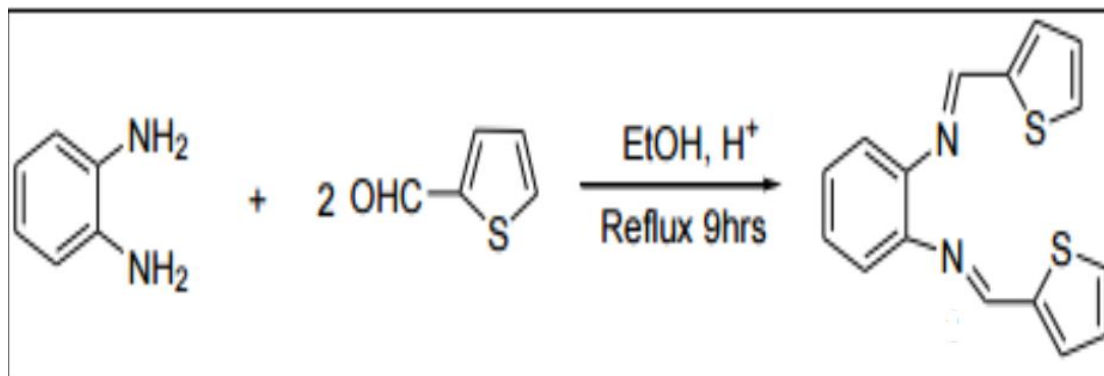
It is very important metal in life, photosynthesis process, mitochondrial respiratory, carbon and nitrogen metabolism, and oxidative stress protection [15].

6. Previous work

There are many previous researches concerted on Schiff base, because of the various importance and uses of the, several type of Schiff bases have been synthesis over the previous years.

I. Reaction of thiophene-2-carbaldehyde with 2-aminoaniline.

This reaction has been carried out by refluxing of thiophene-2-carbaldehyde with 2-aminoaniline in acidic medium using Ethanol as solvent for 9 hours to produce tetradentate NSSN schiff base.



Scheme 2: Reaction of thiophene-2-carbaldehyde with 2-aminoaniline[10]

II. Reaction of thiophene-2-carboxaldehyde with 1,4-diaminocyclohexane to produce Schiff base[**Chart 1**]

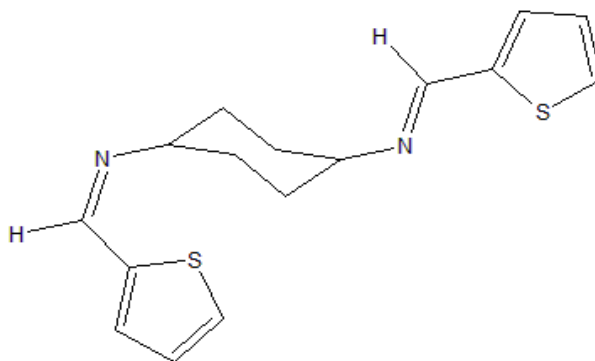


Chart 1 :N,N-bis-thiophen-2-ylm ethylene-cyclohexane-1,4-diamine[10]

III. Reaction of 2-thiophenecarbaldehyde with 1,3-diaminopropane to produce Schiff base [**Chart 2**]

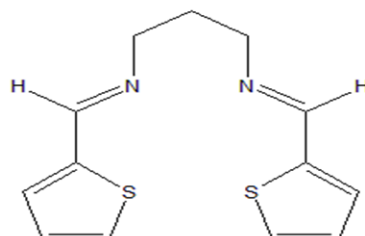


Chart 2: N,N-bis-thiophen-2-ylm ethylene-propane-1,3-diamine[10]

7. Green synthesis, spectral, thermal and X-ray single crystal analysis of 2-(5-bromothiophen-2-yl)-5,5-dimethylhexahydropyrimidineL₁ and their Cu(II) complexes 1-3

Green chemistry focuses on research that attempts to eliminate or reduce the negative environmental impacts [19]. Solvent free reaction have recently received much interest due to many advantages such as: reduced pollution, low costs, simplicity in process and handling, high efficiency and selectivity, purification, easy separation and mild reaction conditions [20]. Moreover, they are not only environmentally safe, but they also are economically beneficial because toxic wastes can be eliminated so that the cost of waste treatment are also reduced.

Hexahydropyrimidines are heterocyclic compounds prepared classically by condensations of substituted propane-1,3-diamines with aldehydes and ketones [21, 22]. Several hexahydropyrimidine derivatives have been prepared and evaluated for many biological activities [23-25] like, antimicrobial [26, 27] leishmanicidal [28] and cytotoxic activities [29], antiviral activity [30] anti-HIV-1 activity [31, 32]. Analgesic activities and anti-inflammatory were also evaluated [33]. Additionally, hexahydropyrimidines were important agents as transport molecules for tumor inhibition and antineoplastic activity [34, 35]. In addition, hexahydropyrimidine are classified as good polydentate ligand for transition metal complexes coordination [36-38]. The interest in hexahydropyrimidine-Metal coordination chemistry has been increasing continuously with the synthesis of a large number of transition metal complexes with heterocyclic

systems containing not only nitrogen, but also O as well as S donor atoms because of their wide applications in various fields pharmaceutical drugs, biological activities [39-41].

It was reported that N5-hexahydropyrimidine ligand coordinated a series of first-row transition metal complexes with several mode of coordination pentadentate to bidentate that depend mainly on the ion metal type and charge [38-45].

As a part of previous researches and in continuation of their ongoing interest in chemistry of novel hexahydropyrimidine derivative [45-47], then study of their complexes coordination and bio-application modes [36, 37].

Chapter Two

Experimental

Chapter Two

Experimental

1. Chemicals

- a. Thiophene-2-carbaldehyde

Formula: C_5H_4SO , Molar mass: 112.14 g/mol, Purity: 99%,

Physical state: liquid, Company: Alfa.

- b. 5-bromothiophene-2-carbaldehyde

Formula: C_5H_3BrSO , Molar mass: 191.04 g/mol, Purity: 99%,

Physical state: liquid, Company: Alfa.

- c. 2,2-dimethyl-propane-1,3-diamine

Formula: $C_5H_{14}N_2$, Molar mass: 102.17 g/mol, Purity: 99%,

Physical state: liquid, Company: Acros.

- d. Cyclohexane-1,2-diamine

Formula: $C_6H_{14}N_2$, Molar mass: 114.18 g/mol, Purity: 99%,

Physical state: liquid, Company: Acros.

- e. Copper(II) Bromide Tetrahydrate

Formula: $CuBr_2 \cdot 4H_2O$, Molar mass: 295.41 g/mol, Purity: 99%,

Physical state: solid, Company: Alfa.

- f. Copper(II) Chloride Dihydrate

Formula: $CuCl_2 \cdot 2H_2O$, Molar mass: 170.48 g/mol, Purity: 99%,

Physical state: solid, Company: Alfa.

- g. Copper(II) Acetate monohydrate

Formula: $C_4H_8CuO_5$, Molar mass: 191.64 g/mol, Purity: 99%,

Physical state: solid, Company: Alfa.

h. Dichloromethane

Formula: CH_2Cl_2 , Molar mass: 84.93g/mol, Purity: 99%, Physical state: liquid, Company: Acros.

i. Hexane

Formula: C_6H_{14} , Molar mass: 86.17 g/mol, Purity: 99%, Physical state: liquid, Company: Acros.

j. Ethanol

Formula: $\text{CH}_3\text{CH}_2\text{OH}$, Molar mass: 46.06 g/mol, Purity: 99%, Physical state: liquid, Company: Acros.

2. Equipments

a. X-Ray diffractometer

Mysore University, India , used to determine the structure of crystalline compound L_1

b. Perkin Elmer Spectrum 1000 FT-IR Spectrometer

Al-Najah National University, Palestine, used to obtain the spectra of resulting ligands L_1 , L_2 and their complexes 1-6

c. TU-1901 double-beam UV–visible spectrophotometer

Al-Najah National University, Palestine used to obtain the maximum wavelength for L_1 and their complexes 1,2

d. NMR Bruker Avance II 400 spectrometer at 298 K, with 5 mm PABBO BB-1H TUBES, using CDCl_3 as a solvent and TMS as internal standard (chemical shift in δ ppm).

Mysore University, India, used to obtain the spectra of resulting ligands L_1 , L_2

- e. TGA-7 PerkinElmer thermogravimetric analyzer (PerkinElmer Inc., Waltham, MA, USA)

Mysore University, India, used to obtain TG/DTG for L_1 , L_2 , and their complexes 1, 4

- f. Thin-layer chromatography using Merck silica gel 60 F254 coated aluminum plates.

Mysore University, India, used to determine the purity of the ligands L_1 , L_2 .

- g. EI-MS

Mysore University, India, used to obtain the spectra for L_1 .

- h. Voltalab 80 potentiostat PGZ402, using H_2O solvent and 0.1M tetrabutyl ammonium hexafluorophosphate (TBAHF) and NH_4Cl supporting electrode.

Mysore University, India, used to obtain the cyclic voltammogram for L_1 and to measure the conductivity for complexes 4-6.

3. Synthesis

3.1. Synthesis of L_1

0.005mol (1g) of 5-bromothiophene-2-carbaldehyde was mixed directly without solvent with 0.005mol (0.53g) of 2,2-dimethyl-1,3-propanediamine in normal test tube. The progress of the reaction was confirmed through the expected increase in temperature and viscosity. The viscous mixture was subjected to ultrasonic vibration at room temperature for 5 min. The produced powder was washed several times with *n*-hexane and then with

water. Finally, the product was recrystallized from dichloromethane, Yield 92%, m.p. 101–105°C.

3.2. Synthesis of L₂

0.008mol (1g) of thiophene-2-carbaldehyde was mixed directly without solvent with 0.009 mol (1.07g) of 1,2-diaminocyclohexane in very small beaker. a significant increase in the reaction's temperature and viscosity has been noticed. The viscous mixture was subjected in ultrasonic vibration at 80 C° for 10 min. Then the solid product was washed with n-hexane.

3.3. Synthesis of complex 1

0.0007mol (0.21g) of L₁ and 0.00071mol (0.21 g) of copper(II) bromide tetrahydrate were dissolved in small amount of ethanol (2 ml), they were mixed together and the colored precipitate has been observed directly. Then the colored product filtered to obtain complex **1**.

3.4. Synthesis of complex 2

0.0007 mol (0.2g) of L₁ and 0.0007mol (0.12g) of copper(II) chloride dihydrate were dissolved in small amount of ethanol (2 ml), they were mixed together and the colored precipitate has been observed directly. Then the colored product was filtered to obtain complex **2**.

3.5. Synthesis of complex 3

0.0007 mol (0.2g) of L₁ and 0.0007mol (0.14g) of Copper(II) acetate monohydrate were dissolved in small amount of ethanol (2 ml), they were

mixed together and the colored precipitate has been observed directly. Then the colored product was filtered to obtain complex **3**.

3.6. Synthesis of complex 4

6.6×10^{-4} mol (0.2 g) of L_2 and 6.6×10^{-4} mol (0.19 g) of copper bromide tetrahydrate were dissolved in ethanol (2ml), then they were mixed together and the color change has been observed after the mixture was subjected to ultrasonic vibration at 80°C for 10 min. Then ethanol was removed to obtain complex **4**.

3.7. Synthesis of complex 5

6.6×10^{-4} mol (0.2 g) of L_2 and 6.4×10^{-4} mol (0.11g) of Copper(II) chloride dehydrate were dissolved in ethanol, then they were mixed together and the color change has been observed after the mixture was subjected to ultrasonic vibration at 80°C for 10 min. Then ethanol was removed to obtain complex **5**.

3.8. Synthesis of complex 6

6.6×10^{-4} mol (0.2g) of L_2 and 6.5×10^{-4} mol (0.13 g) Copper(II) acetate were dissolved in small amount of ethanol, then they were mixed together and the color change has been observed after the mixture was subjected to ultrasonic vibration at 80°C for 10 min. Then ethanol was removed to obtain complex **6**.

Chapter Three

Results and Discussion

Part One

Part One

Green synthesis, spectral, thermal and X-ray single crystal analysis of 2-(5-bromothiophen-2-yl)-5,5-dimethylhexahydropyrimidineL₁ and their Cu(II) complexes 1-3

1. Single Crystal X-ray Diffraction

Single crystals suitable for X-ray diffraction study were obtained by a slow evaporation technique using dichloromethane as a solvent. A white coloured rectangular shaped single crystal of dimensions 0.3×0.27×0.25 mm of the title compound was chosen for an X-ray diffraction study. The X-ray intensity data were collected at a temperature of 296 K on a Bruker Proteum2 CCD diffractometer equipped with an X-ray generator operating at 45 kV and 10 mA, using CuK_α radiation of wavelength 1.54178 Å. Data were collected for 24 frames per set with different settings of $\varphi(0^\circ$ and $90^\circ)$, keeping the scan width of 0.5° , exposure time of 2 s, the sample to detector distance of 45.10 mm and 2θ value at 46.6° . A complete data set was processed using *APEX 2* [48]. The structure was solved by direct methods and refined by full-matrix least squares method on F^2 using *SHELXS* and *SHELXL* programs [49]. All the non-hydrogen atoms were revealed in the first difference Fourier map itself. All the hydrogen atoms were positioned geometrically and refined using a deriding model. After ten cycles of refinement, the final difference Fourier map showed peaks of no chemical significance and the residuals saturated to 0.0566. The geometrical

calculations were carried out using the program *PLATON* [33]. The molecular and packing diagrams were generated using the software *MERCURY* [34]. The details of the crystal structure and data refinement are given in **Table 1**.

The list of bond lengths and bond angles of the non-hydrogen atoms are given in **Table 2**. **Figure 11** represents the ORTEP of the molecule with thermal ellipsoids drawn at 50% probability.

Table 1: Crystal data and structure refinement details

Empirical formula	C ₁₀ H ₁₅ BrN ₂ S		
Formula weight	275.21		
Temperature	296(2) K		
Wavelength	1.54178 Å		
Refins. for cell determination	1807		
θ range for above	4.17° to 64.26°		
Crystal system	Monoclinic		
Space group	<i>P</i> 21/ <i>c</i>		
Cell dimensions			
$a = 6.0492(2)$ Å	$b = 21.2238(8)$ Å	$c = 9.3452(4)$ Å	
$\alpha = 90.00^\circ$	$\beta = 106.5190(10)^\circ$	$\gamma = 90.00^\circ$	
Volume	1150.28(8) Å ³		
<i>Z</i>	4		
Density(calculated)	1.589 Mg m ⁻³		
Absorption coefficient	6.268 mm ⁻¹		
F_{000}	560		
Crystal size	0.25 × 0.25 × 0.25 mm		
θ range for data collection	4.17° to 64.26°		
Index ranges	-7 ≤ <i>h</i> ≤ 4		
	-24 ≤ <i>k</i> ≤ 22		
	-8 ≤ <i>l</i> ≤ 10		
Reflections collected	5535		
Independent reflections	1870 [$R_{\text{int}} = 0.0499$]		
Absorption correction	multi-scan		
Refinement method	Full matrix least-squares on F^2		
Data / restraints / parameters	1870 / 0 / 129		
Goodness-of-fit on F^2	1.128		
Final [$I > 2\sigma(I)$]	$R1 = 0.0566$, $wR2 = 0.1529$		
<i>R</i> indices (all data)	$R1 = 0.0576$, $wR2 = 0.1553$		
Largest diff. peak and hole	1.073 and -1.343 e Å ⁻³		

2.Synthesis

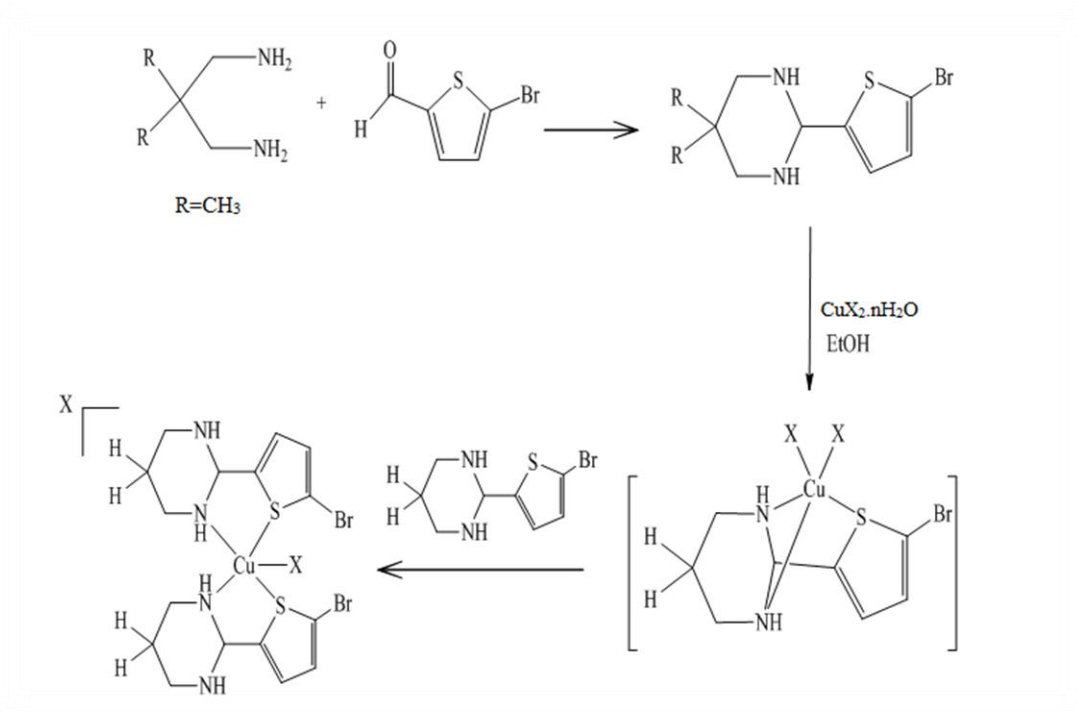
2.1. Synthesis of L₁

The Solvent-free reaction scheme for the synthesis of L₁ is depicted in **Scheme 4**. The white product was obtained in an excellent yield by direct solvent-free condensation of 5-bromothiophene-2-carbaldehyde and 2,2-dimethyl-1,3-propanediamine. And that's where both reactants are liquid in nature, the mixing together enabled the interaction to occur quickly without side product. The reaction was confirmed by heat and viscosity raised upon mixing of reactants. L₁ was solid and soluble in CH₂Cl₂, partially in ROH, insoluble in water and non-polar solvents like *n*-hexane. Similar to Evans [52], who studied the 1,3-diaminopropane cyclization with formaldehyde, we have no indications that the tautomeric open-chain product is formed, the only isolable product was hexahydro-5-methyl-5-(pyridin-2-yl) pyrimidine. We also found that: for complete cyclization process without side products excess of aldehyde should be added.

2.2. Synthesis of complexes 1-3.

Complexation of L₁ with copper(II) halide and acetate happens readily, and is carried out by direct mixing both of L₁ with Cu(II) in 1: 2 stoichiometric amounts using ethanol solvent. The colored Cu(II) salt dissolved in methanol turn to green directly upon addition of 1:1 [L₁:Cu(II)] then to blue when more ligand was added, this suggested the formation of [L₁CuX₂] as unstable intermediate followed by [(L₁)₂CuX]X final product, as shown in **Scheme 4**, the complexes **1-3** are slightly soluble in EtOH and insoluble in water which

confirms the non-cationic nature. The coordination mode around the Cu(II) center adopted by the tridentate chelate ligands of both of amine nitrogen atoms of **L**₁ ring and sulfur of the thiophene-2-carbaldehyde which are coordinated to the copper center. Five coordination number around the copper was expected without any water or solvent molecule coordination.



Scheme 4: Synthesis of **L**₁ and their complexes **1-3**

3. EI-MS of **L**₂

The elemental analysis of the free ligand is consistent with the proposed molecular formula (Calcd. for C₁₀H₁₅BrN₂S: C, 43.64; H, 5.49; N, 10.18. Found: C, 43.45; H, 5.41; N, 10.25%).

TOF-MS of **L**₁ is in good agreement with the assigned structure and showed the experimental molecular ion [M⁺] *m/z* = 275.0 (275.2 theoretical), and the peak at 273.0793 due to Bromine isotope (⁷⁹Br).

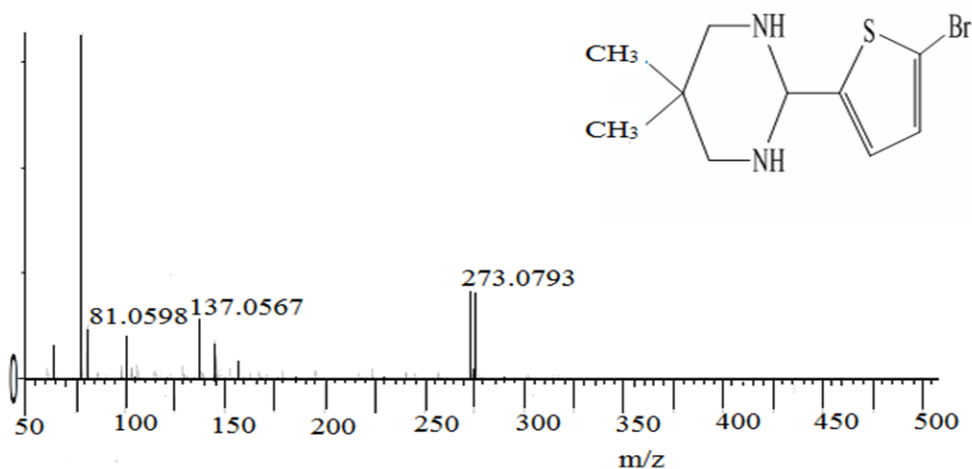


Figure 1: TOF-MS spectrum of L₁

4. Frontier molecular orbital analysis of L₁

Knowledge of the highest occupied molecular orbital (HOMO) and lowest unoccupied molecular orbital (LUMO) and their properties such as their energy is very useful to gauge the chemical reactivity of the molecule. The ability of the molecule to donate an electron is associated with the HOMO and the characteristic of the LUMO is associated with the molecule's electron affinity [53, 54].

The electronic absorption corresponds to the transition from the ground to the first excited state described by one electron excitation from the HOMO to the LUMO. The pictorial representation of the HOMO and the LUMO in the gaseous phase is shown in **Figure 2**. HOMO lies at -0.2155 eV and whereas LUMO is located at -0.0180 eV with frontier orbital energy gap of 0.2 eV. It is more easily that the electrons are excited from the ground to the excited state with this low energy gap. The energy gap explains the eventual

charge transfer interaction within the molecule and it uses in determining molecular electrical transport properties.

By using the HOMO and LUMO energy values, the global chemical reactivity descriptors such as hardness, chemical potential, electronegativity and electrophilicity index as well as local reactivity can be defined [50–54].

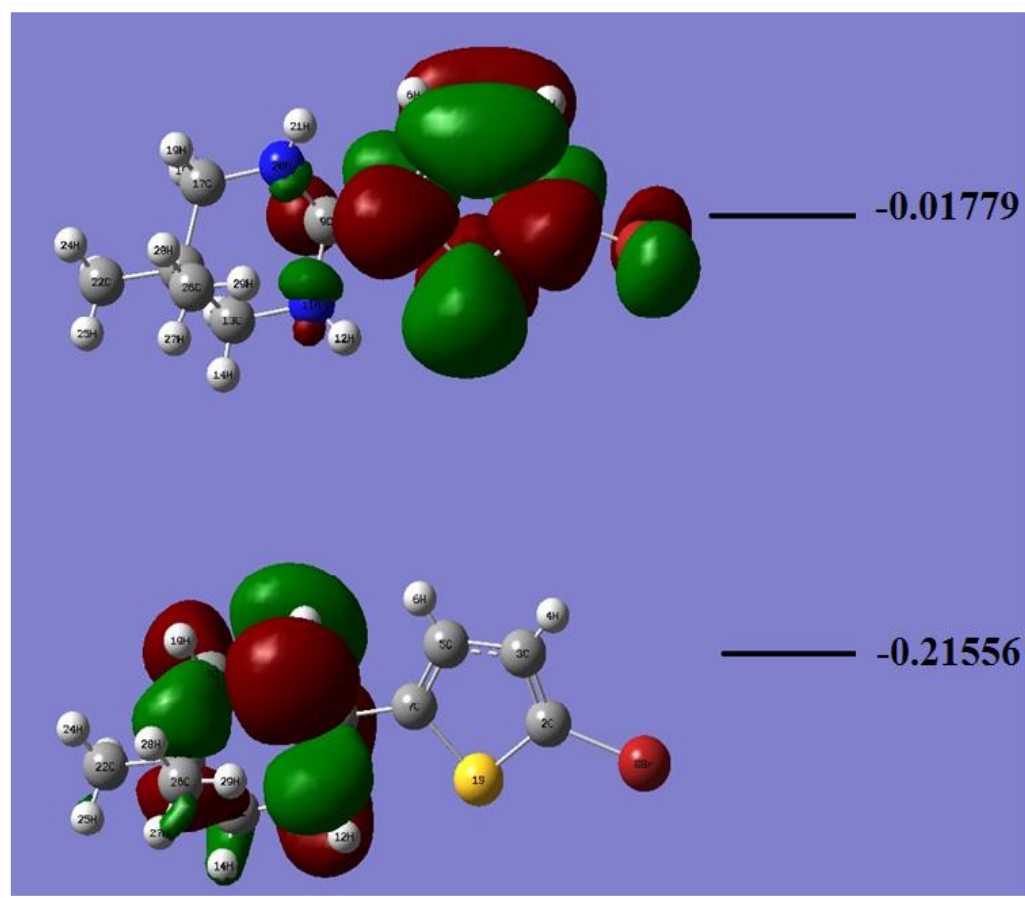


Figure 2: HOMO and LUMO plots of L_1

5. UV-Vis Spectral Analysis of L_1 and their complexes 1-2

The electronic absorption spectra for L_1 and their complexes 1-2 are measured in ethanol at room temperature, and the experimental absorption bands are assigned using the time-dependent DFT method. The spectrum of

L₁ exhibits high intense transitions at $\lambda_{max} = 245$ nm which is due to $\pi-\pi^*$ electron transition (see **Figure 3a**).

The ultraviolet spectral analysis of **L**₁ have been investigated by TD-DFT/B3LYP/3-311++G method. Calculations of molecular orbital geometry show that the visible absorption maxima of this molecule correspond to the electron transition between frontier orbitals such as transition from HOMO to LUMO. As can be seen from the UV-vis spectra the values of absorption maxima was found to be 250 nm (See **Figure 3b**). There is a good match between the experimental measurements compared with the theoretical and perhaps these values that may be slightly shifted by solvent effects (see **Figure 3b**).

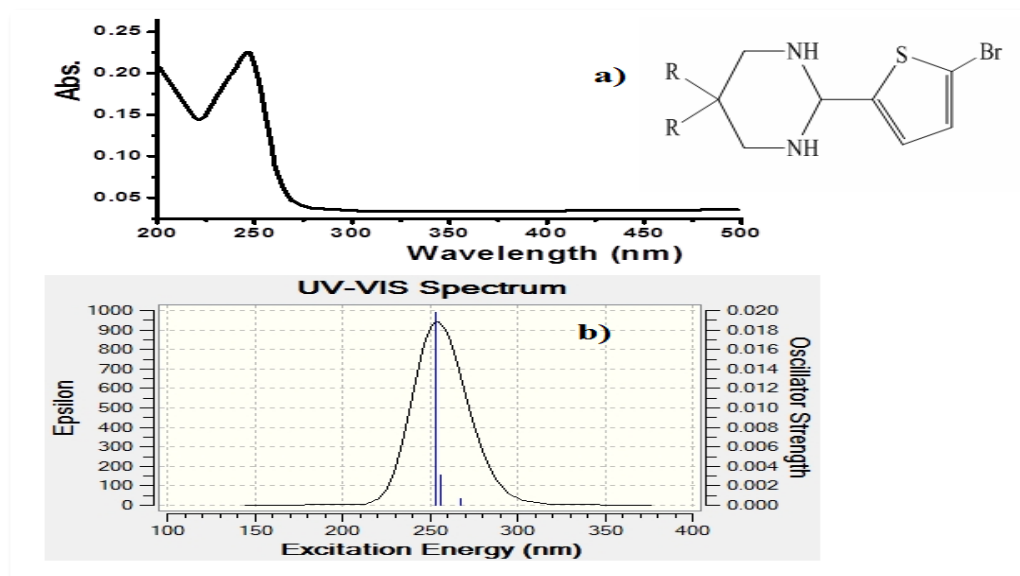


Figure 3: UV-Vis spectra of **L**₁ ethanol at room temperature a), TD-DFT/B3LYP/3-311++G UV-vis method b).

The electronic spectra of complexes **1** and **2** in ethanol shows additional bands in the visible regions 600-650 nm which is attributed to $[\text{Cu}(\text{L}_1)_2\text{X}]\text{X}$ monocation complexes formation (see **Figure 4**).

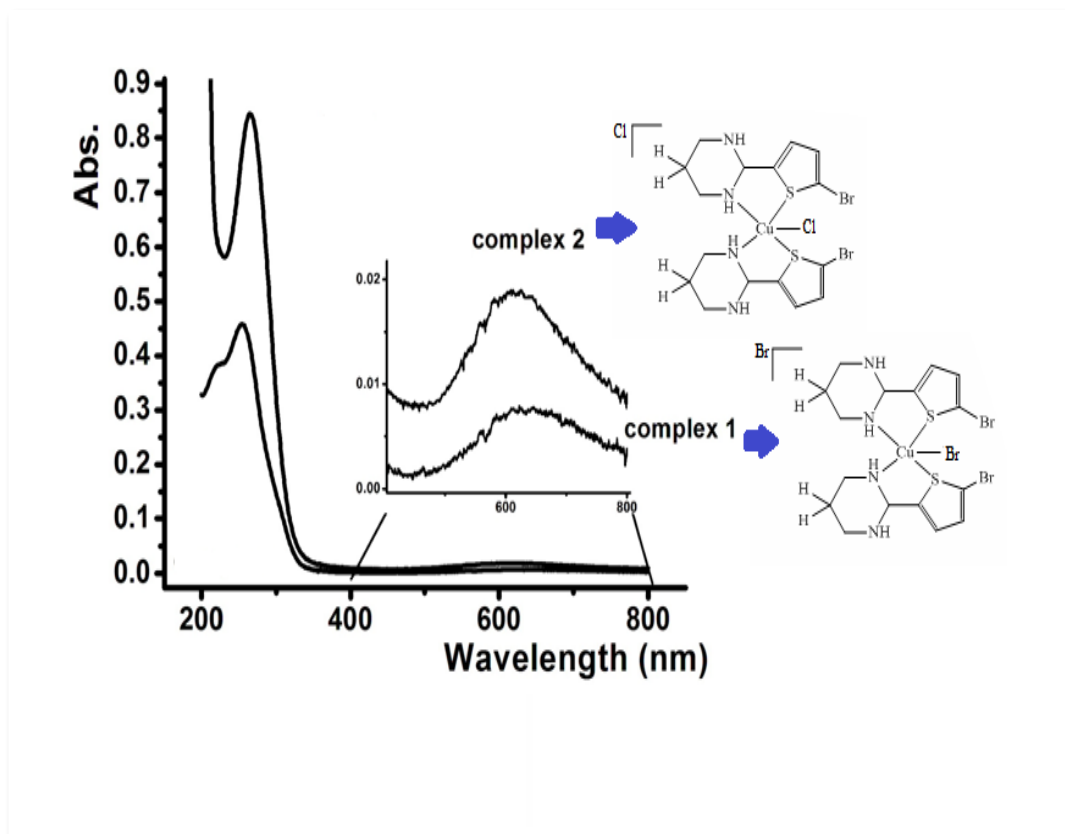


Figure 4: UV–Vis spectra of complexes **1** and **2** dissolved in EtOH at RT.

Inherently, the green color complexes which were formed due to [1:1] of CuX_2 to the ligand L_1 addition (which were suggested to be for the neutral $[\text{CuL}_1\text{X}_2]$) revealed bands in the visible regions 650-700 nm. These bands were shifted to lower wavelengths (600-650 nm) by addition one more L_1 due to the formation of stable monocation $[\text{Cu}(\text{L}_1)_2\text{X}]\text{X}$ complexes (see **Figure 5**).

Such visiblebands in both CuL_1X_2 or $[\text{Cu}(\text{L}_1)_2\text{X}]\text{X}$ complexes are not recorded in the spectra of the free ligand nor in CuX_2 and are attributed to d to d electron transfer of square planer geometry around Cu(II) center.

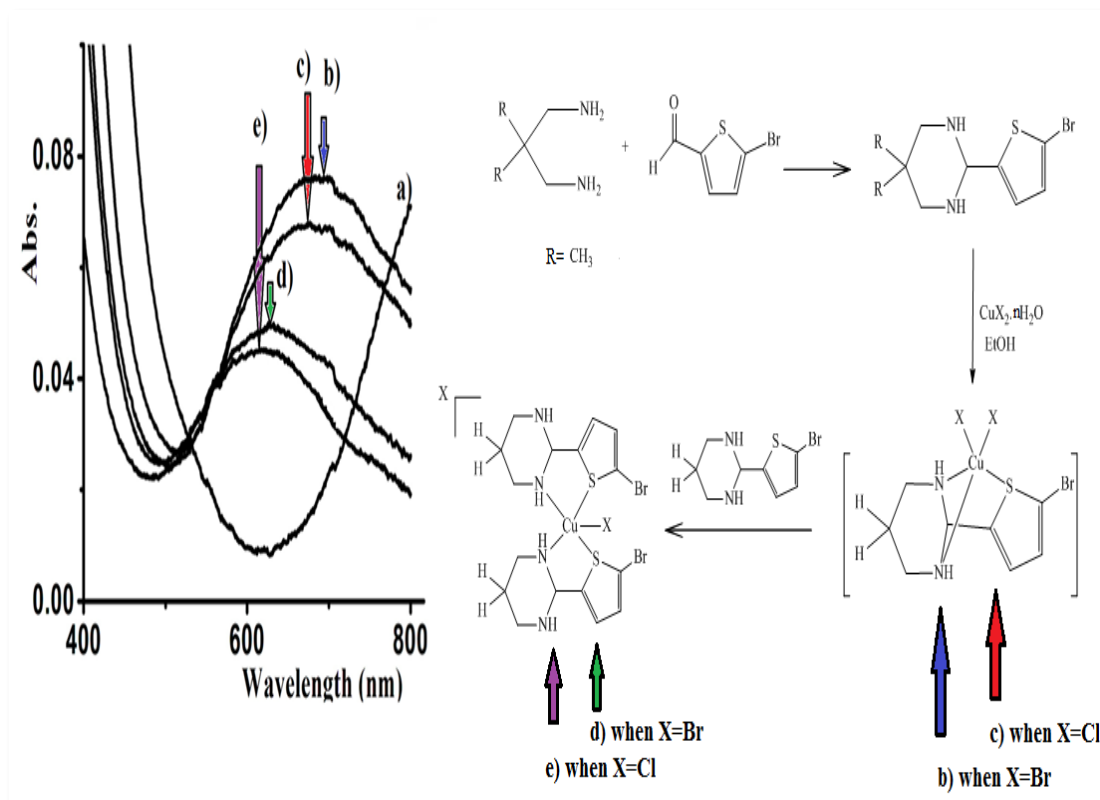


Figure 5: In situ Vis-spectra of a) free CuBr_2 , b) CuL_1Br_2 , c) CuL_1Cl_2 , d) $[\text{Cu}(\text{L}_1)_2\text{Br}]\text{Br}$ and e) $[\text{Cu}(\text{L}_1)_2\text{Cl}]\text{Cl}$ dissolved in EtOH at RT.

6. FT-IR Spectral Analysis

6.1. FT-IR Spectral Analysis of L_1

FT-IR of L_1 was investigated In order to control the solvent-free condensation reaction of 5-bromothiophene-2-carbaldehyde and 2,2-dimethyl-1,3-propanediamine the reaction was monitored by FT-IR (see **Figure 6**).

The starting materials were subjected to IR before and after it mixing to produce L_1 .

The formation of **L**₁ was confirmed by three major changes: the primary N-H bond stretching vibration in 2,2-dimethyl-1,3-propanediamine at 3400 and 3450 cm⁻¹ (see **Figure 6a**) which was reduced to single vibration at 3250 cm⁻¹, due to the formation of secondary amine of **L**₁ (see **Figure 6c**). Stretching vibrations of C=O and CH-aldehyde in 5-bromothiophene-2-carbaldehyde were appeared at 1745 and 3120 cm⁻¹ respectively. Such vibrations were disappeared due to **L**₁ formation (see **Figure 6b and c**).

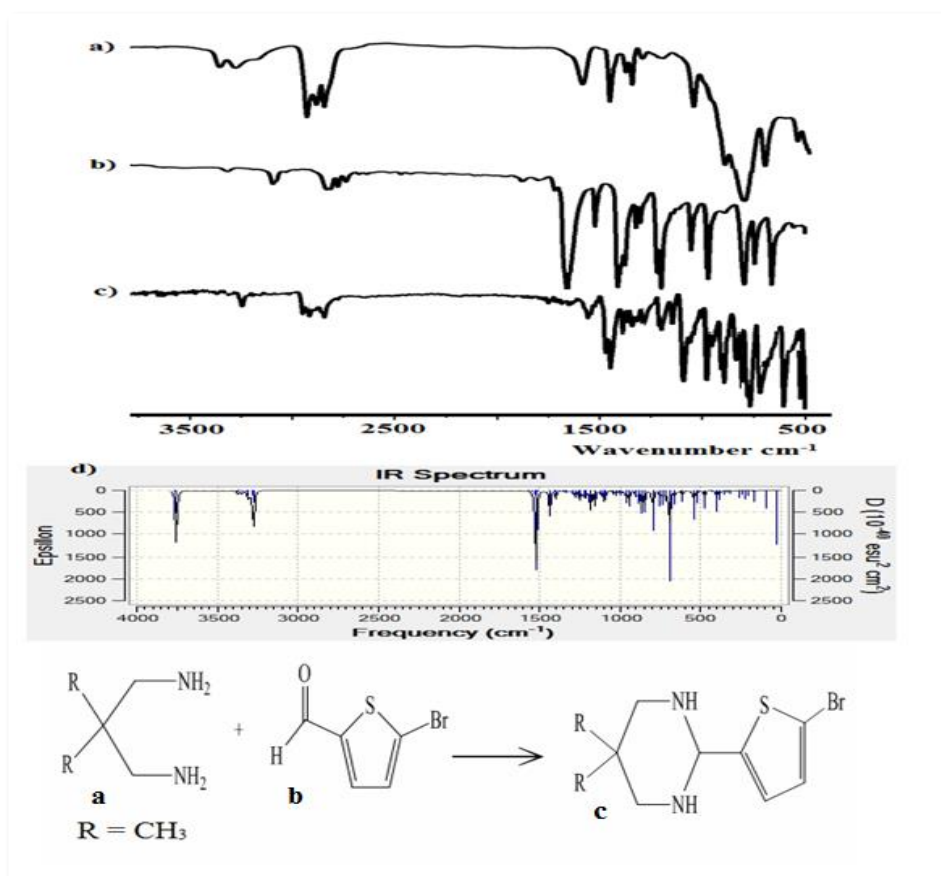


Figure 6: IR spectra of: a) 2,2-dimethyl-1,3-propanediamine, b) 5-bromothiophene-2-carbaldehyde and c) **L**₁, d) calculated with B3LYP/3-311+G.

The most significant absorption bands of **L₁** were shown in **Figure 6c**. at 3250, 3000, 2850–2950 cm^{-1} . Such band can be assigned to N-H, aromatic C–H, aliphatic C-H stretching vibrations, respectively.

For visual comparison, the observed FT-IR spectrum of **L₁** was compared with theoretical one and DFT/B3LYP level using 3-311+G basis set(look up **Figure 6 c and d**), respectively. The calculated frequencies are slightly higher than the observed value for the majority of normal modes. The major factor which is responsible for these discrepancies between the experimental and the computed value is related to the fact that the experimental value is an harmonic frequency while the calculated value is an unharmonic frequency [55].

6.2. FT-IR of complex 1-2

The IR spectrum of the isolated complexes **1-2** showed several functional groups vibrations: The NH stretching frequency bands in the complexes **1-2** are observed at 3150-3250 cm^{-1} as doublet. The singlet stretching vibration NH in **L₁** was converted to doublet in complexes due to the losing in the symmetry around the metal confirmed the following facts: only one of NH is coordinated to copper center as seen in **Scheme 3**. The observed shift in values towards the shorter wave number region can be also accounted to the Cu-N coordination. It can be concluded that **L₁** behaves as a bidentate ligand, via one of their S and one N atoms . The spectra of the complexes show new absorption bands in the range of 700-500 cm^{-1} range assigned to $\nu(\text{Cu-S})/\nu(\text{Cu-N})$, (see **Figure 7**)

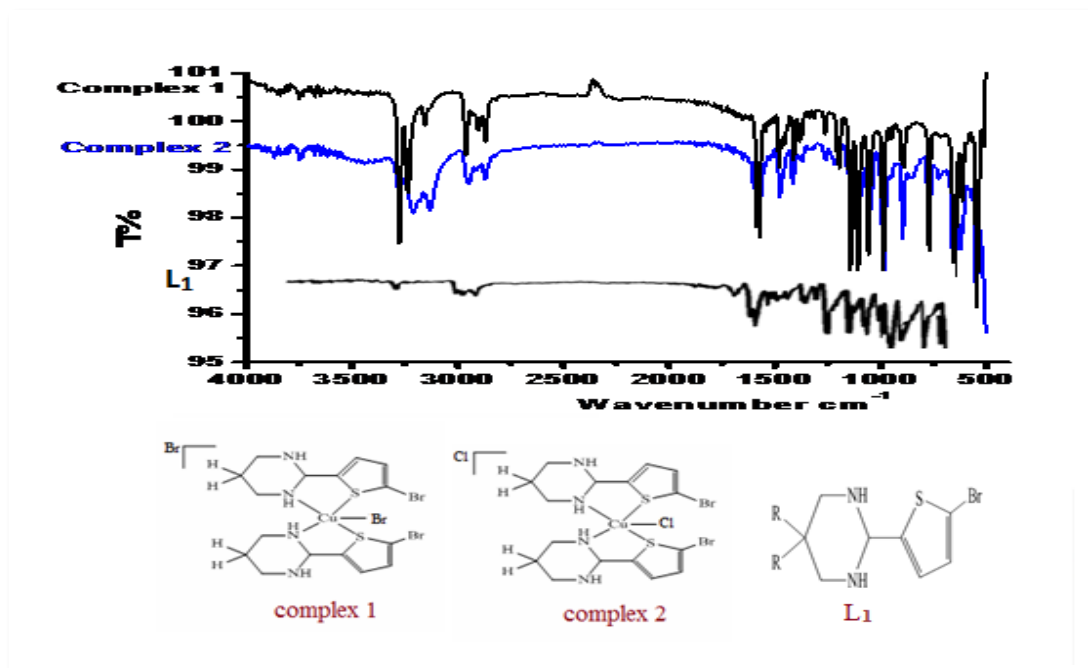


Figure 7: FT-IR spectrum of complex 1-2 and L₁

7. Thermal analysis investigation of L₁

The thermal properties TG/DTG of L₁ (see **Figure 8a**) and complex 1 (see figure 8b) have been performed under an open atmosphere in the range of 0–900 °C with heating rate of 10 °C/min.

Figure 8a shows the TG curve of L₁ which exhibits a remarkable thermal stability at about 100 °C. The compound decomposes to light gases like: CO₂, SO₂, NO₂ in one broad step (100% Wt lost). A typical decomposition, started from ~110 °C and end at ~250°C, with no intermediate decomposition steps or remaining residue, was recorded.

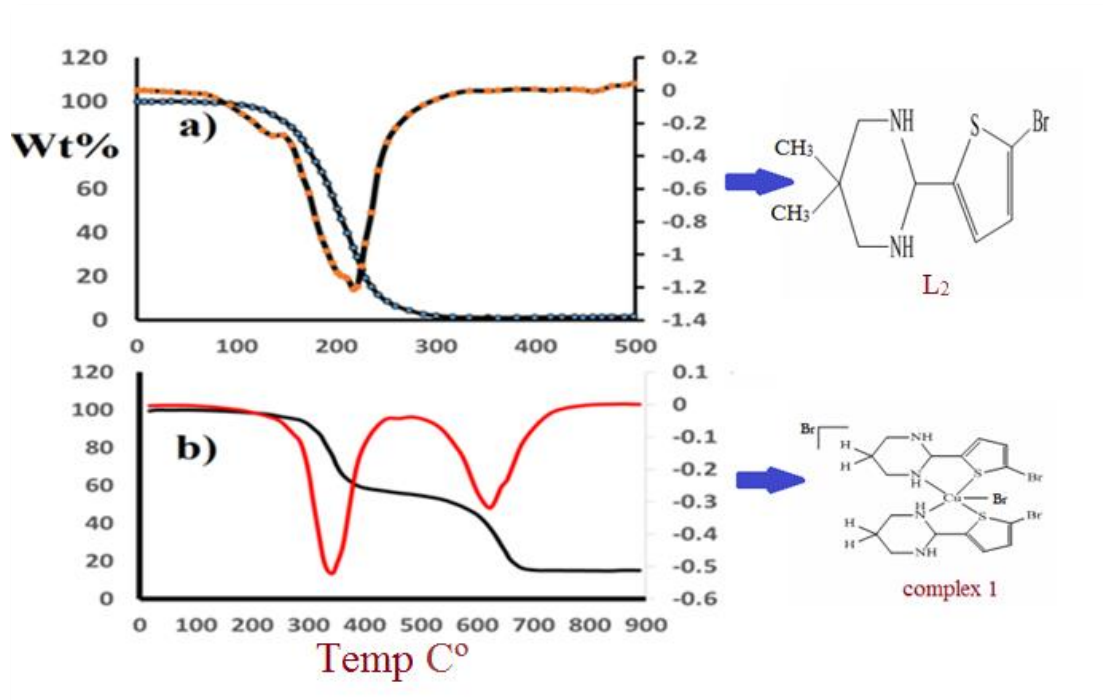


Figure 8: TG/DTG thermal curves of the L₁ a) and of the complex 1 b).

The thermogram of complex 1 is characterized by two degradation steps in the range 280-390 °C, 580-700 °C (see **Figure 8b**), the first step corresponding to elimination and/or decomposition of L₁ to form CuBr₂, and the second step can be attributed to the elimination of two Br to form CuO as final product, the final product was confirmed by IR.

8. ¹H and ¹³C NMR spectral analysis of L₁

The ¹H NMR spectrum of L₁ shown in **Figure 9** ¹H NMR spectrum showed two sharp broad singlets at δ 0.85 and 1.5 ppm are due to 2CH₃ protons. A broad singlet at δ 1.78 ppm is due to 2NH protons.

A broad singlet at δ 2.85 ppm is due to 2CH₂ protons. A sharp Singlet at δ 4.62 ppm is due to CH proton. The two aromatic protons resonated as a multiplet in the region of δ 6.70–7.00 ppm.

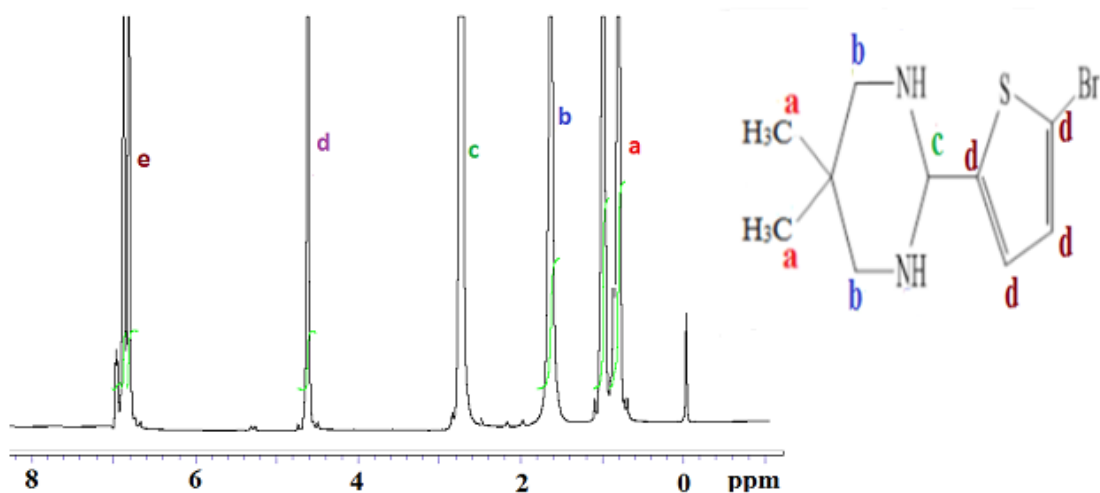


Figure 9: ^1H NMR spectrum of **L1** dissolved in CDCl_3 at RT

In ^{13}C NMR spectrum showed two signals at δ 22.6 and 25.9 ppm due to 2CH_3 , singlet at δ 56.8 ppm due to 2CH_2 , Singlet at δ 69.8 ppm due to CH, The four aromatic carbons resonated as singlets at δ 111.5, 123.9, 129.5, 147.9 ppm (see **Figure 10**).

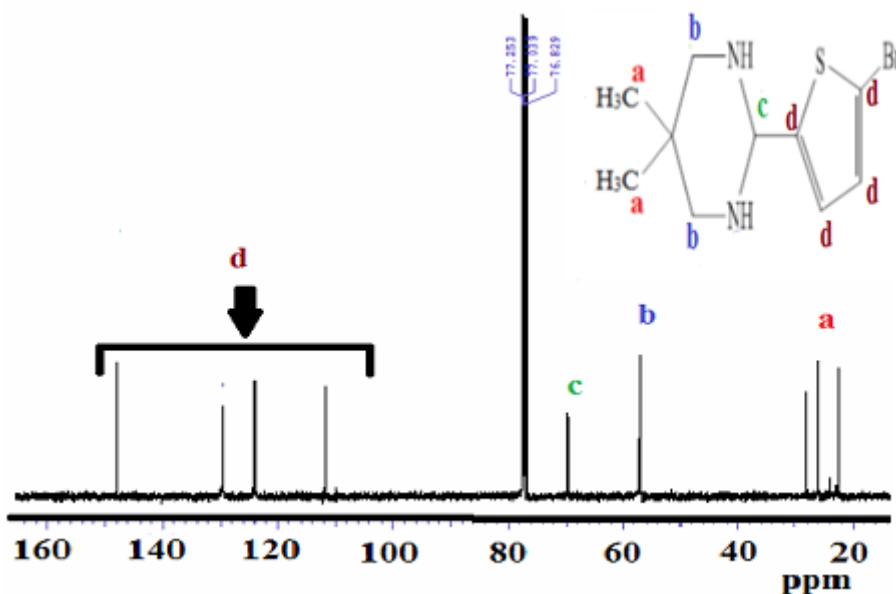


Figure 10: ^{13}C NMR spectrum of **L1** dissolved in CDCl_3 at RT

9. X-ray structural determination investigation of L₁

A study of torsion angles, asymmetric parameters and least-square plane calculations reveals that the six-membered hexahydropyrimidine ring adopts a chair conformation. The atoms C7 and C10 are deviating 0.182(4) Å and -0.224(4) Å respectively from the Cremer and Pople plane [56] which are defined by the atoms N8/C9/C11/N12. This is confirmed by the puckering parameters $Q = 0.508(4)$ Å, $\theta = 173.6(5)^\circ$ and $\phi = 108(4)^\circ$. The bonds C7-C5 and C10-C13 make an angle of $69.6(2)^\circ$ and $62.9(2)^\circ$ respectively with the Cremer and Pople plane of the hexahydropyrimidine ring and thus are in equatorial plane of the hexahydropyrimidine ring. The bond C10-C14 makes an angle of $7.5(2)^\circ$ with respect to the hexahydropyrimidine ring and this lies in the axial plane, (see **Figure 11** and **Table 2** and **3**). The bond lengths and bond angles are normal and the molecular conformation is characterized by a dihedral angle of $21.21(18)^\circ$ between the mean planes of the two aromatic rings indicating that they are twisted with respect to each other. The molecular conformation is stabilized by both inter and intramolecular N—H...S hydrogen bonds which tend to form a *S(6)* ring motif. The packing of the molecules when viewed down along the *c* axis indicates that the molecules exhibit layered stacking and are interlinked by the hydrogen bond to form a one dimensional chain like structure (see **Figure 12**).

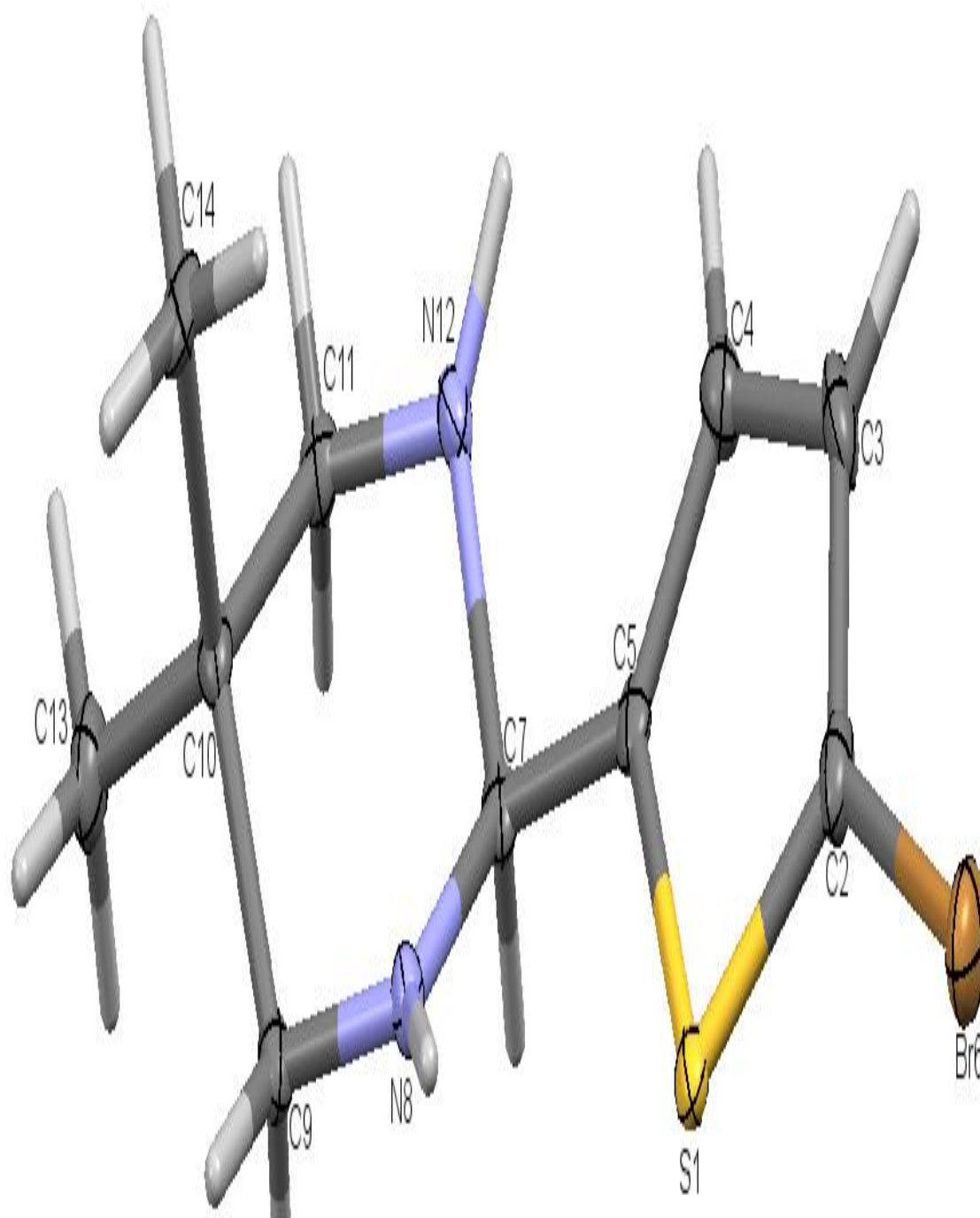


Figure 11: ORTEP diagram of L1 with thermal ellipsoids drawn at 50% probability.

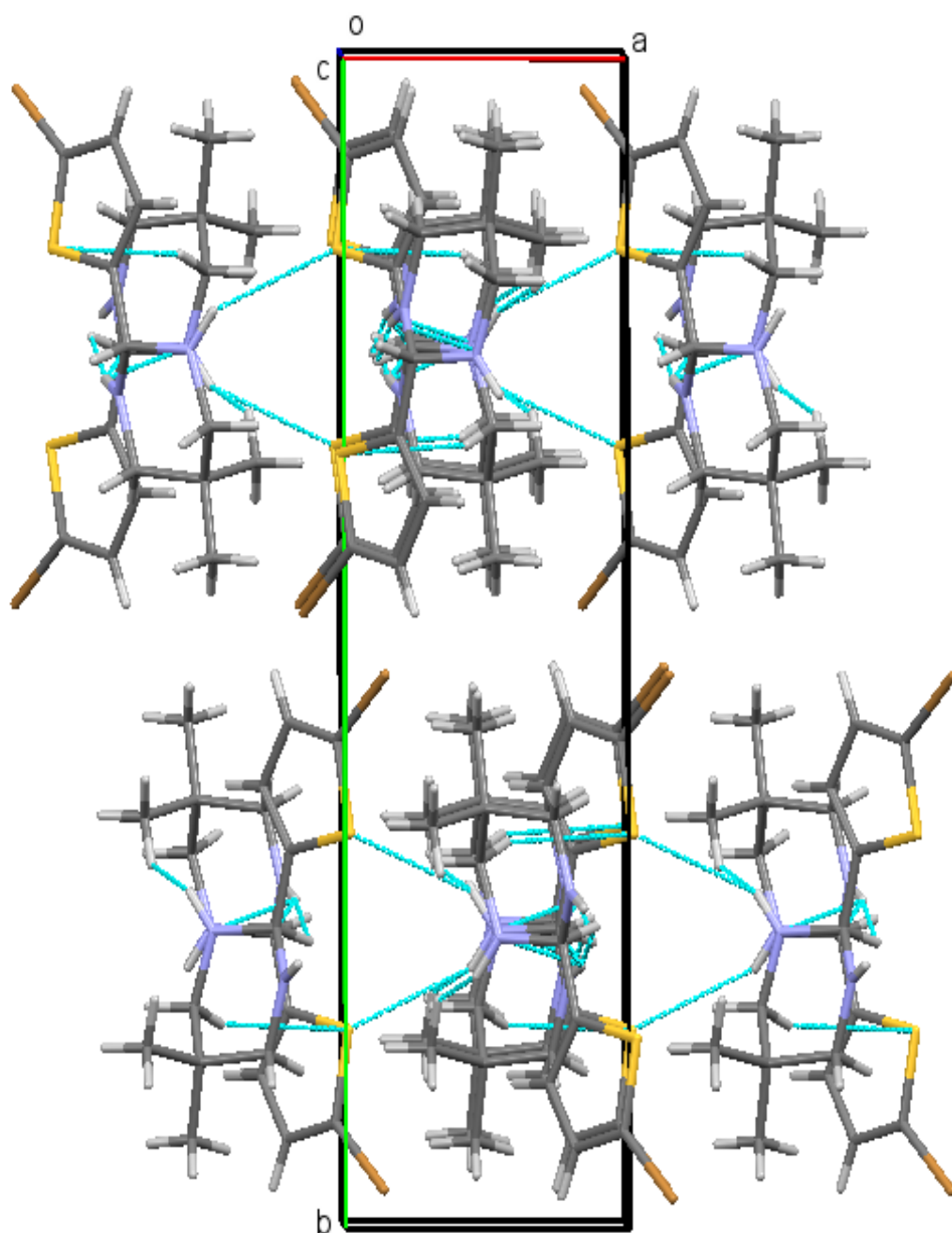


Figure 12: Packing of L_1 molecules when viewed down along the c -axis indicating layered stacking

Table 4: Bond lengths (Å).

Atoms	Length	Atoms	Length
S1-C2	1.723(4)	C7-N8	1.462(5)
S1-C5	1.734(4)	N8-C9	1.466(5)
C2-C3	1.362(6)	C9-C10	1.535(5)
C2-Br6	1.874(4)	C10-C13	1.520(5)
C3-C4	1.422(6)	C10-C14	1.537(5)
C4-C5	1.354(5)	C10-C11	1.538(5)
C5-C7	1.501(5)	C11-N12	1.471(5)
C7-N12	1.457(5)		

Table 5: Bond angles (°)

Atoms	Angle	Atoms	Angle
C2-S1-C5	91.10(18)	N8-C7-C5	109.9(3)
C3-C2-S1	112.7(3)	C7-N8-C9	110.2(3)
C3-C2-Br6	127.3(3)	N8-C9-C10	114.2(3)
S1-C2-Br6	120.0(2)	C13-C10-C9	109.7(3)
C2-C3-C4	111.1(3)	C13-C10-C14	109.7(3)
C5-C4-C3	114.3(4)	C9-C10-C14	111.1(3)
C4-C5-C7	129.7(3)	C13-C10-C11	108.5(3)
C4-C5-S1	110.9(3)	C9-C10-C11	107.4(3)
C7-C5-S1	119.5(3)	C14-C10-C11	110.4(3)
N12-C7-N8	116.7(3)	N12-C11-C10	115.0(3)
N12-C7-C5	109.4(3)	C7-N12-C11	112.1(3)

10. Hirshfeld surface analysis of L₁

Hirshfeld surface analysis is an effective tool for exploring packing modes and intermolecular interactions in molecular crystals. They offer a visual picture of intermolecular interactions and of molecular shape in a crystalline environment. Surface feature characteristics of different types of intermolecular interactions can be identified and these features can be

revealed by color coding distances from the surface to the nearest atom exterior (d_e plots) or interior (d_i plots) to the surface. This gives a visual picture of different types of interactions present, and also reflect their relative contributions from molecule to molecule. Further, 2D fingerprint plots, in particular the breakdown of 2D fingerprint plots into specific atom...atom contacts in a crystal, provide a quantitative idea of the types of intermolecular contacts experienced by molecules in the bulk and presents this information in a convenient color plot. Hirshfeld surfaces comprising d_{norm} surface plots, electrostatic potential and 2D fingerprint plots were generated and analyzed for the **L1** in order to explore the packing modes and intermolecular interactions, and to demonstrate the efficiency of this tool in demonstrating the crystal structure of the compound to the surface.

Hirshfeld surface analyses were carried out and finger print plots were plotted using CrystalExplorer 3.0 [57]. Electrostatic potentials were calculated using TONTO [58, 59]. The d_{norm} plots were mapped with color scale in between -0.18 au (blue) and 1.4 au (red). The electrostatic potential is mapped on the Hirshfeld surface using STO3G basis set at the Hartree–Fock theory over the range of ± 0.025 au.

The two dimensional fingerprint plots from Hirshfeld surface analyses (see **Figure 13**), illustrates the difference between the intermolecular interaction patterns and the relative contributions to the Hirshfeld surface (in percentage) for the major intermolecular contacts associated with the title compound. Importantly, H...H (49.3%) bonding appears to be a major contributor in the crystal packing followed by C...H (13%), S...H(12.2%) and

N...H(1.4%) bonds thereby revealing the information regarding the intermolecular N--H...S hydrogen bonds. These observations are further confirmed by the respective electrostatic potential maps (see **Figure 14**) in which the atoms involved in the formation of strong hydrogen bonds are seen as dark-blue (hydrogen bond donor) and dark-red spots (hydrogen bond acceptors) whereas the atoms involved in the weaker interactions are seen as light-blue or light-red spots.

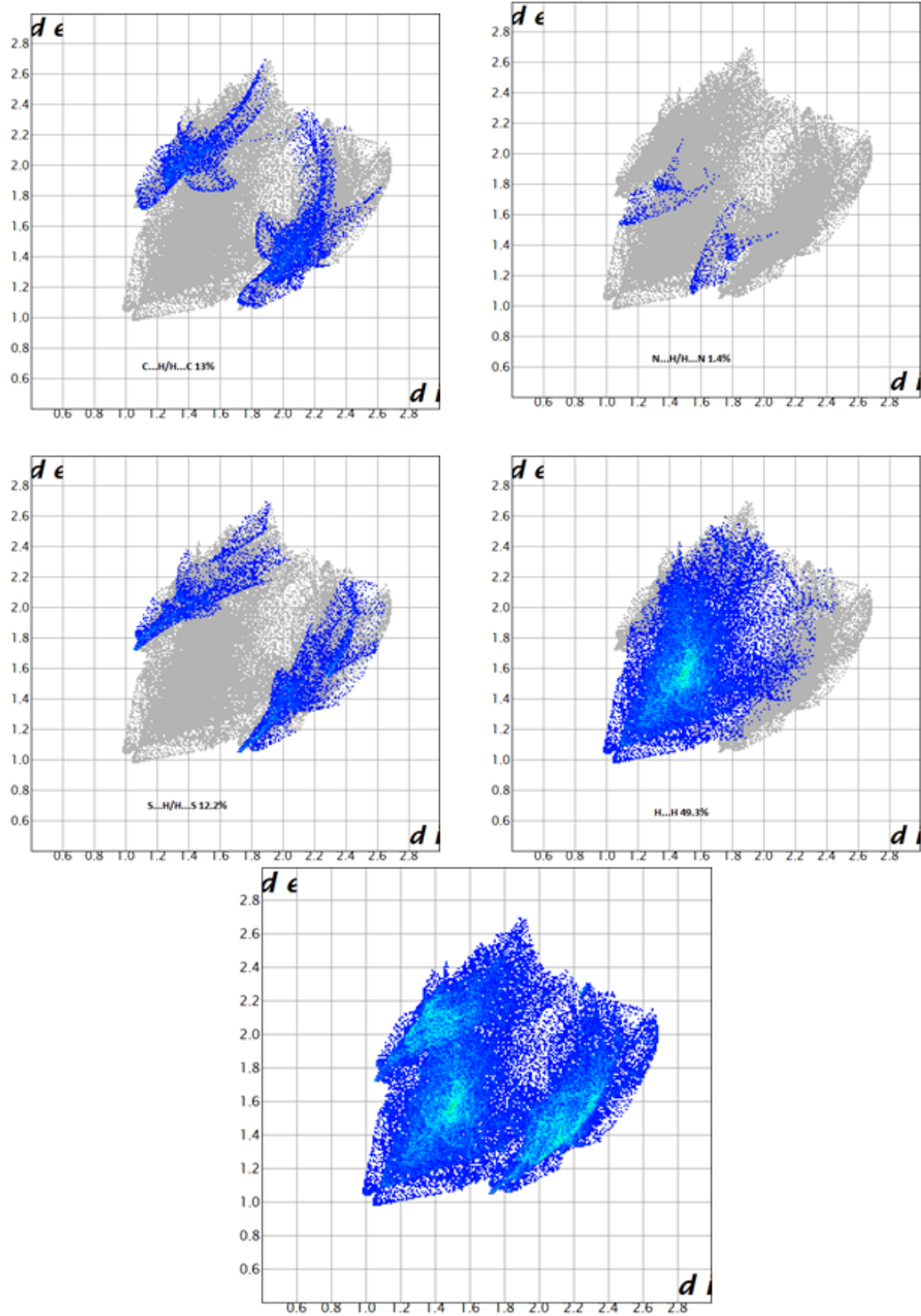


Figure 13:Fingerprint plots of L_1

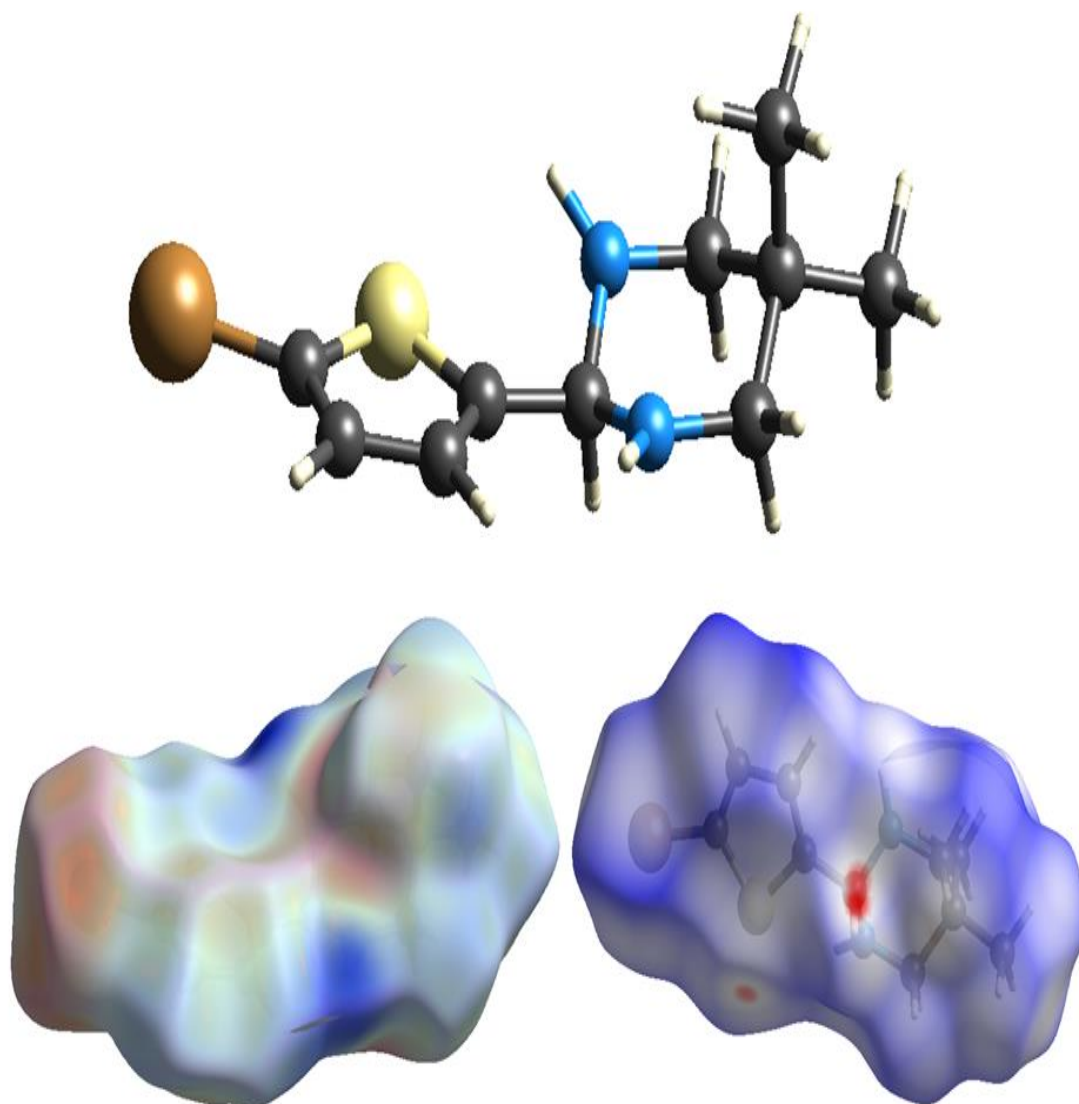


Figure 14: d_{norm} and electrostatic potential mapped on Hirshfeld surface for visualizing the intermolecular contacts. The ball and stick models represent the different orientations corresponding to the Hirshfeld surface and the electrostatic potential

11. Conclusion

L₁ was synthesized for the first time by solvent-free condensation of 5-bromothiophene-2-carbaldehyde with 2,2-dimethyl-1,3-propanediamine at mild condition. The new ligand was fully characterized by EI-MS, FT-IR spectroscopy, TG/DTA, Uv-visible, ¹H, ¹³C-NMR and finally the structure was confirmed by X-ray diffraction and Hirshfeld surface analysis studies. **L**₁ crystallizes in the monoclinic crystal system with the space group *P*2₁/*c* space group with crystal parameters of *a* = 6.0492(2) Å, *b* = 21.2238(8) Å, *c* = 9.3452(4) Å, β = 106.5190(10)°, *V* = 1150.28(8) Å³ and *Z* = 4. The condensation reaction was monitored by FT-IR and compared by DFT theoretical calculation.

L₁ was served as bidentate and tridentate ligand when subjected to CuX₂ salt to prepare monocation water soluble [Cu(**L**₁)₂X]X (X = Cl, Br and OAc) complexes 1-3 (see charts 13, 14, 15).

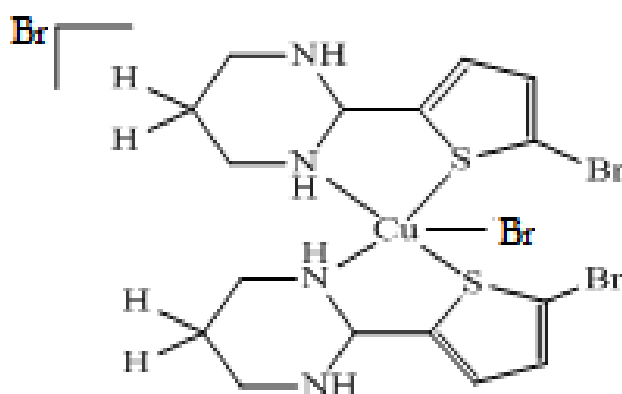


Chart 3: Expected structure of complex 1

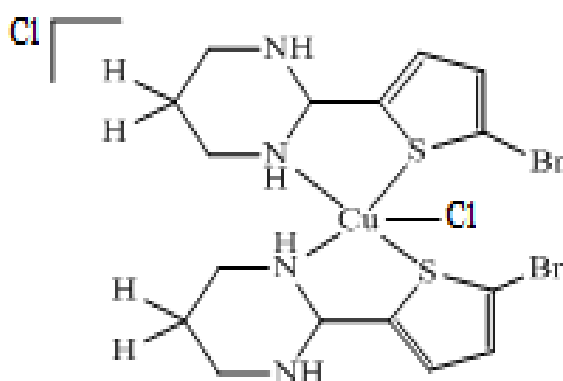


Chart 4: Expected structure of complex 2

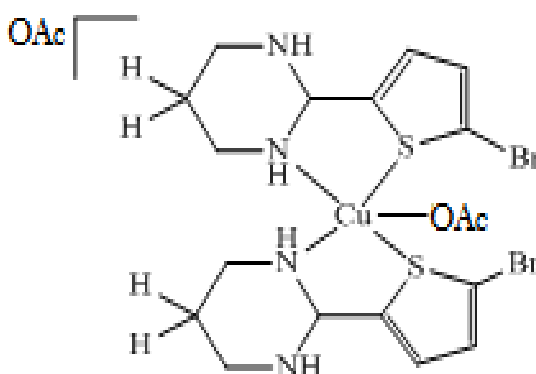


Chart 5: Expected structure of complex 3

The isolated complexes were spectrally characterized using FT-IR spectroscopy.

The resulting product was not as we expected, surprisingly, the reaction changed their direction towards the formation of cyclic compound instead of Schiff base formation.

A 6-member ring was obtained as a final product since such ring is thermodynamically and kinetically stable.

This phenomenon is observed in 1,3-diamine and not in 1,2-diamine compounds, such finding was observed when we applied green chemistry strategy instead of harsh conditions strategy.

Part Two

Part Two

Synthesis, Spectral and Thermal studies of N,N-bis-thiophene-2-ylmethylene-cyclohexane-1,2-diamine and their Cu(II) complexes.

1. Synthesis

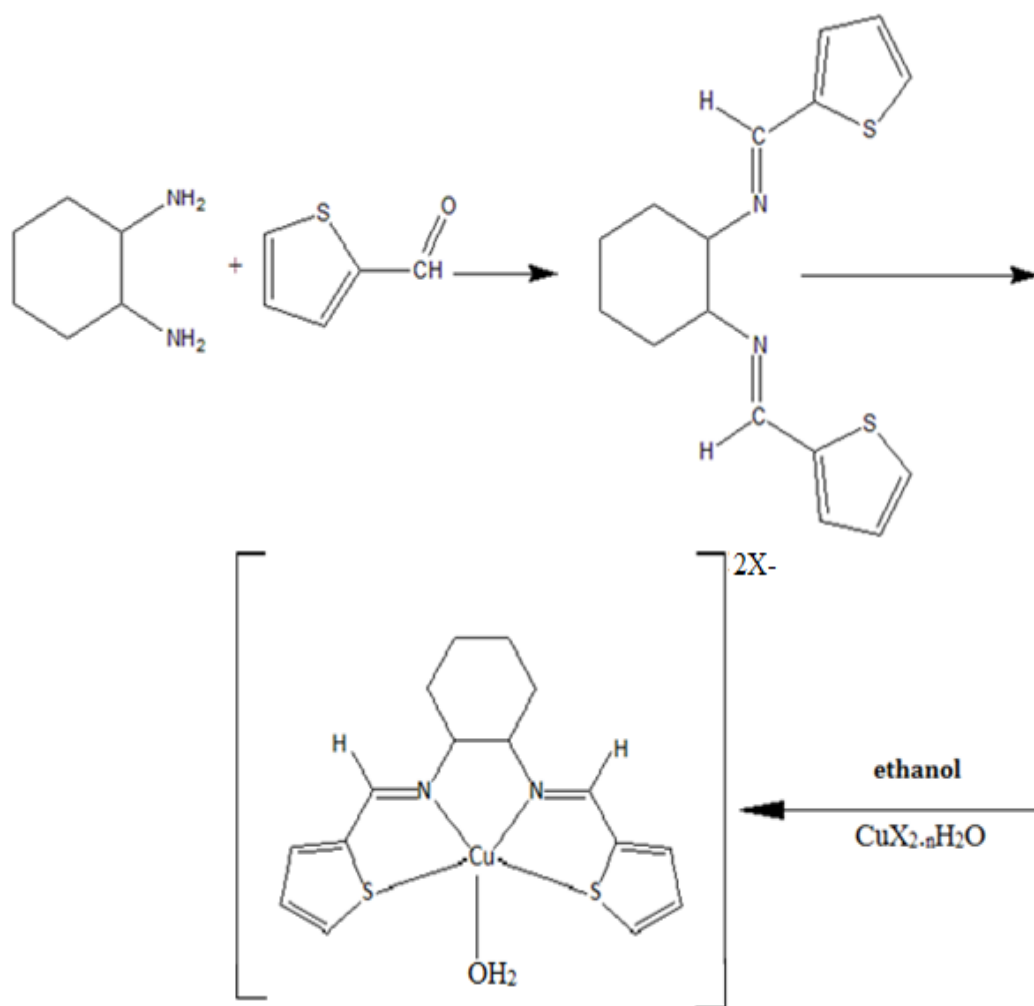
1.1. Synthesis of L₂

A pale yellow product was obtained by direct and fast reaction of thiophene-2-carbaldehyde and cyclohexane-1, 2-diamine.

Mixing of the two compound enabled the reaction to occur quickly without side product. The reaction was confirmed by heat and viscosity raised upon mixing of reactants. The product L₂ was solid and soluble in CH₂Cl₂, partially in EtOH, insoluble in water and non-polar solvents like *n*-hexane. The structure of L₂ was confirmed by FT- IR ,¹H NMR spectroscopy.

1.2. Synthesis of complexes 4-6

The direct reaction scheme for the synthesis of **complexes 4-6** is shown in **Scheme 4**. The blue products were obtained in an excellent yield by direct and fast reaction of L₂ with copper chloride, bromide and acetate in the presence of ethanol as a solvent. The reaction was confirmed by color changing and solid formation when mixing of L₂with CuX₂ , where X = Br, Cl, OAc. L₂ was totally soluble in H₂O, and they are insoluble in CH₂Cl₂.



Scheme 4: synthesis of **L₂** and their complexes **4-6**

2. FT-IR spectral analysis

2.1. FT-IR of **L₂** and starting materials

FT-IR was investigated in this study to monitor the condensation reaction of thiophene-2-carbaldehyde and cyclohexane-1,2-diamine.

The starting materials were subjected to IR before and after mixing to produce **L₂**, the formation of **L₂** was confirmed by: Primary amine stretching vibration in cyclohexane-1,2-diamine at 3350 and 3450cm^{-1} was

disappeared (see **Figure 15a**), due to the formation of tertiary amine (see **Figure 15c**).

Stretching vibrations of C=O and CH of 5-bromothiophene-2-carbaldehyde at 1655 and 3155 cm^{-1} respectively, and the stretching of C=O was shifted to 1627 cm^{-1} due to C=N of **L₂** (see **Figure 15** and **Figure 15c**).

The most significant absorption bands of **L₂** is were shown in **Figure 15c** at 2995, 2850–2950 cm^{-1} region. Such bands can be assigned to aromatic C–H, aliphatic C-H stretching vibrations, respectively.

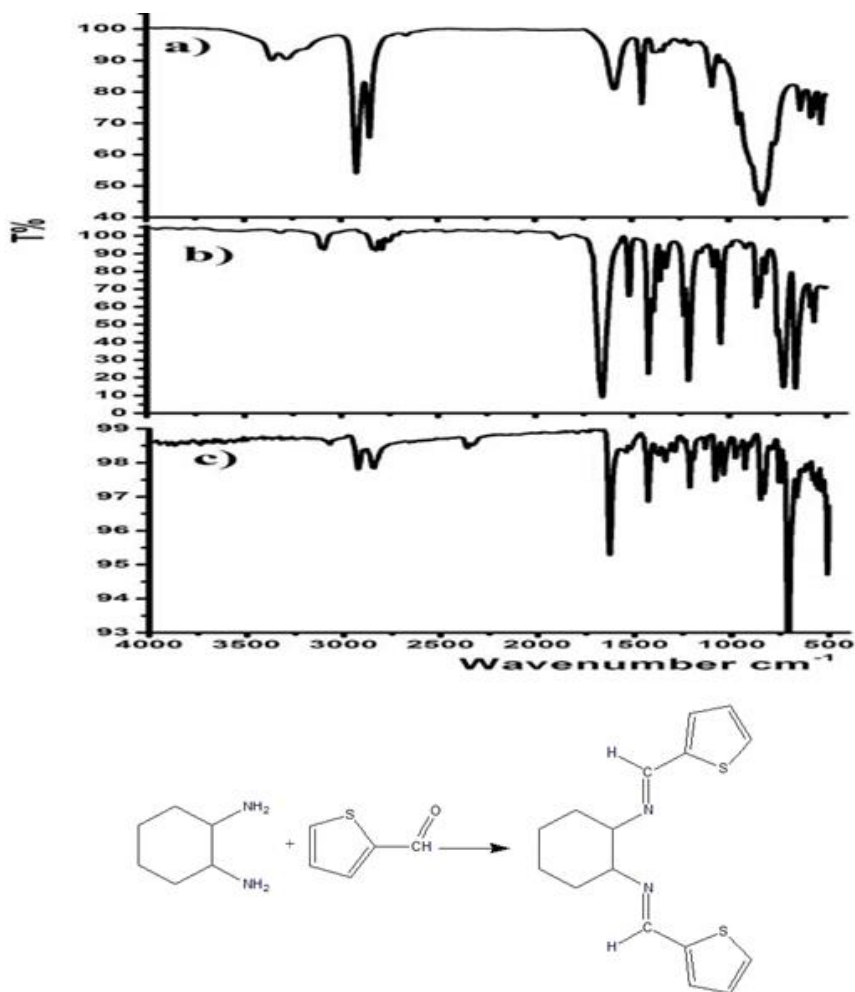


Figure 15: IR-spectrum for a) Cyclohexane-1,2-diamine, b)thiophene-2-carbaldehyde,c) **L₂**

2.2. FT-IR of L_2 and their complexes 4-6

The following notes are due to IR:

Strange sharp peaks from 3300 to 3350 cm^{-1} for complexes 1-2 and this observations support H_2O direct coordination to Cu(II) center, such suggestion was supported by several physical measurements.

- 1) Solubility in water. Solubility of complexes was found to be very high in water.
- 2) electric conductivity.

It was 180 $\mu\text{s}/\text{m}$, which fit with dicationic more than monocationic form.

In general all the complexes revealed several stretching vibrations for aromatic C-H at 3066 cm^{-1} , and aliphatic C-H at 2800 and 2900 cm^{-1} . In addition complex **3**

show broad in the range of 3100- 3750 cm^{-1} due to adsorption of water. (see **Figure 16c**) All complexes revealed several new vibrations in the range of 500 - 700 cm^{-1} , due to Cu-N and Cu-S.

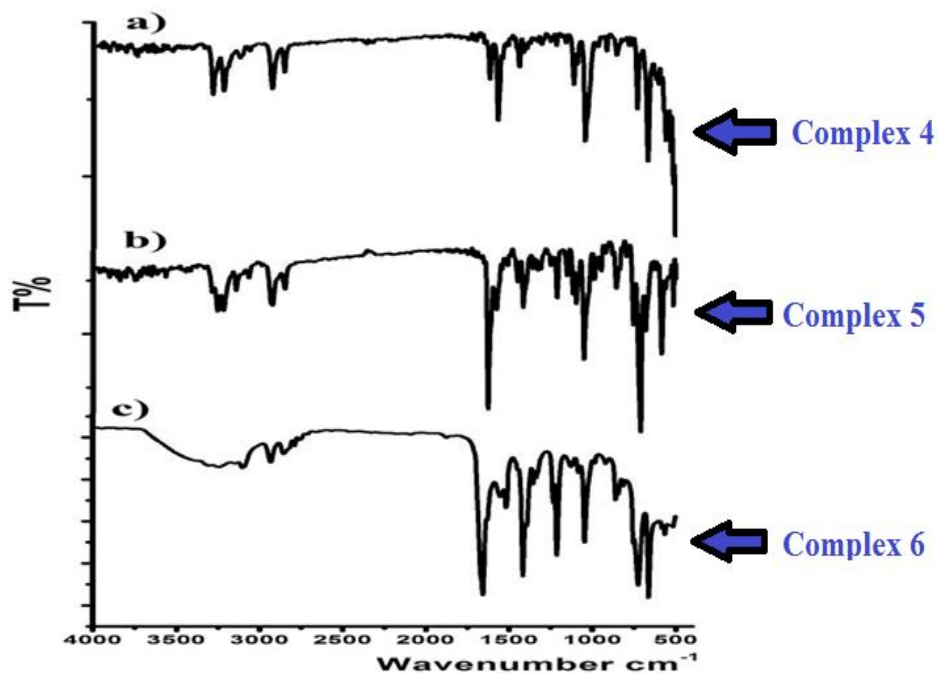


Figure 16 : IR-spectrum for, a)Complex 4, b)Complex 5, c)Complex 6

The prepared **complexes 4-6** here in this section are expected to have two cationic general formula, monocationic complex, which has formula of $[(L_1)_2CuX]X$, in which one of the halide atom coordinated to copper center and dicationic complexes, which has the formula of $[(L_1)_2CuH_2O]X_2$, in which the two halides atom are spectator ions. (See **Chart 6**)

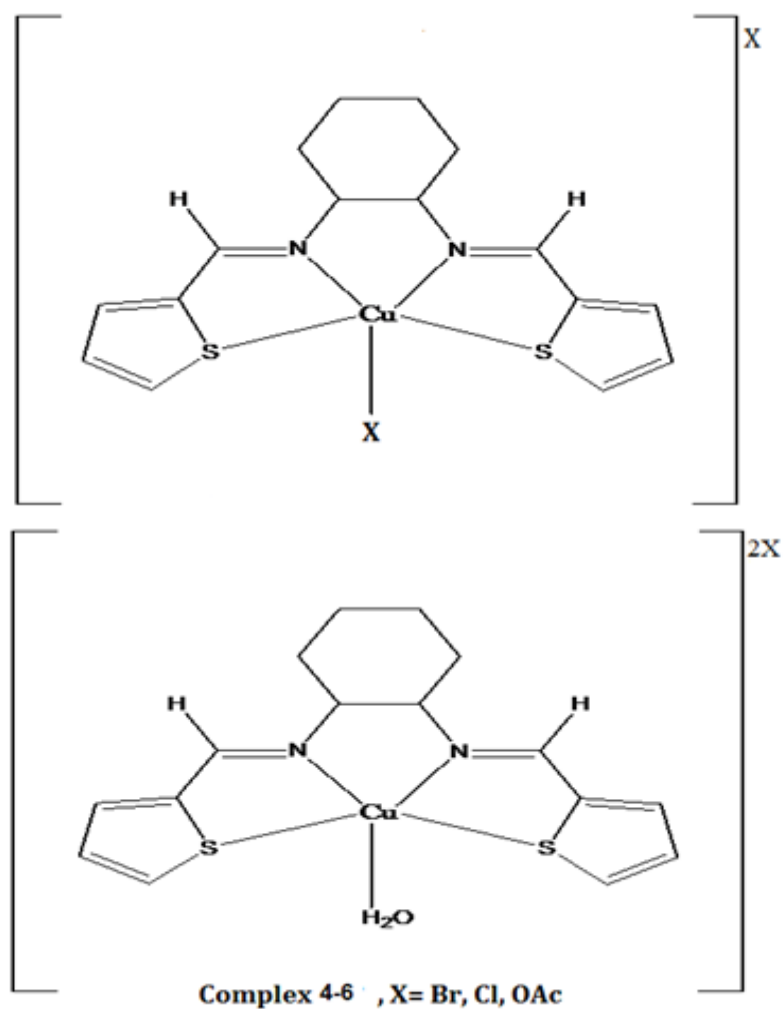


Chart 6: Monocationic and dicationic complexes.

It is very difficult to differentiate between both monocationic and dicationic form, just by IR, which was confirmed the formation of dicationic. The observing bands in the range of $3300-3350\text{cm}^{-1}$, due to coordinated water molecule.

3. NMR Spectral Analysis of L₂

3.1. ¹H NMR spectral analysis of L₂

The ¹H NMR spectrum of L₂ was carried out to characterize the final product. The two multiplet signals at 1.3 to 1.9 ppm were due to 4CH₂ of aliphatic cycle(cyclohexane-1,2-diamine), the multiplet signal at 3.4 ppm was due to 2CH of aliphatic cycle, the several multiplet in the range of 6.7- 7.4 ppm were due to CH of thiophene ring, and finally the singlet at 8.3ppm was due to CH of C=N (see **Figure 17**).

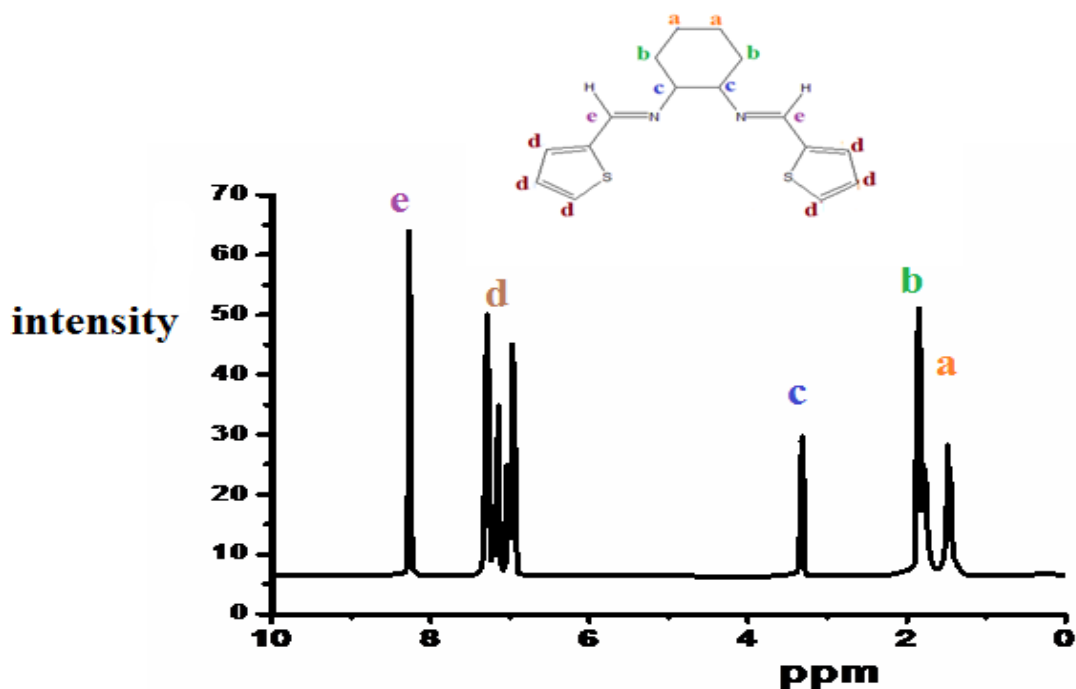


Figure 17: ¹H NMR spectrum of L₂ dissolved in CDCl₃ at RT.

3.2. ^{13}C NMR spectral analysis of L_2

^{13}C NMR spectrum of L_2 was carried out to characterize the final product. The chemical shift at 25 and 32 ppm are due to 4C of cyclohexane, and they have been mentioned with the letters a and b, the signal at 74 ppm due to another two Carbon of cyclohexane and it has been mentioned with the letter c, the four signal in the range of 126-131 ppm are due to carbons of thiophene ring and they have been mentioned with the letters d,e,f, and h, the last one at 155 ppm is due to carbon of C=N. (see **Figure 18**)

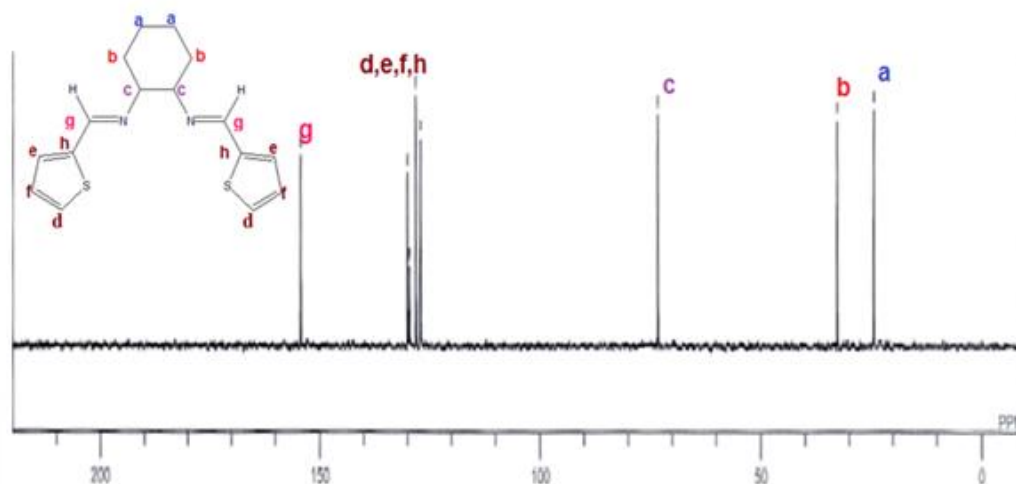


Figure 18: ^{13}C NMR spectrum of L_2 dissolved in CDCl_3 at RT.

4. Cyclic Voltammetry of complex 5

The electrochemical behaviour of **complex 5** were investigated by cyclic voltammetry in DMF solutions containing 0.1 M of TBAPF₆ as supporting electrolyte. Cyclic voltammograms were recorded at different scan rate 0.1V vs Ag/AgCl.

The experimental results proved that the reduction of **complex 5** proceed through a quasi-reversible one electron process with unity anodic to cathodic current (I_{pa}/I_{pc}) ratio, generating the Cu(I) species, which has a life time long enough to be detected by cyclic voltammetry as it is illustrated in **Figure 19**.

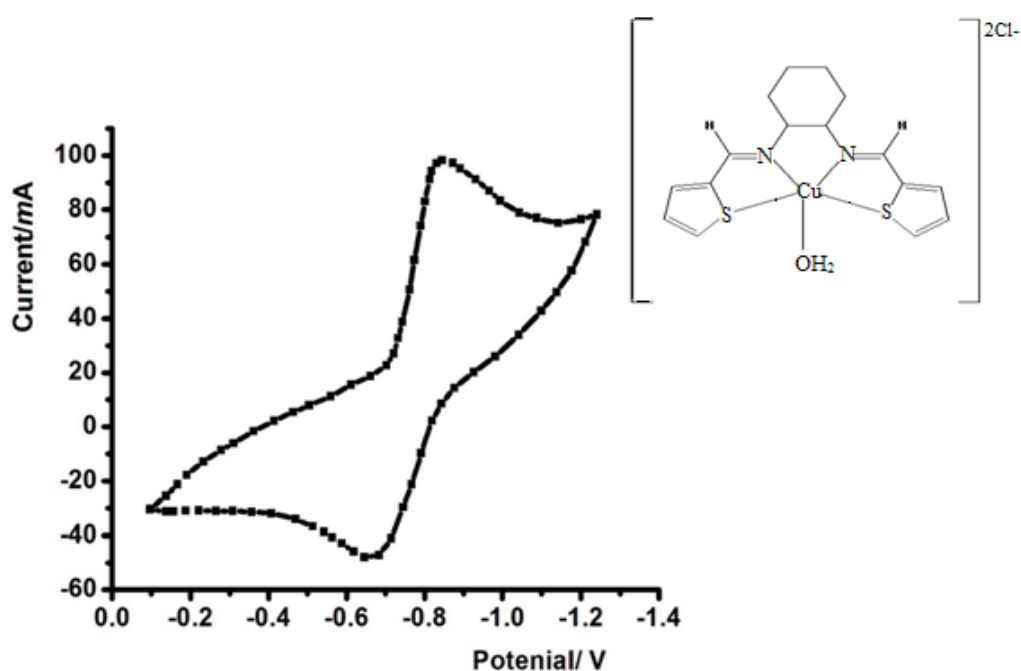
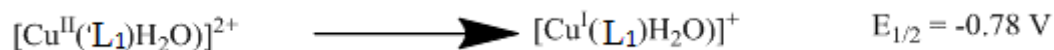


Figure 19: Cyclic voltammogram of complex **5** in DMF solution, at scan rates 0.1 V/s

The redox process can be formulated as follows:



The quasi-reversibility associated with the reduction process probably arises as a consequence of a geometry change from the originally square pyramidal towards a distorted tetrahedral environment around the Cu(I) species [60].

5. Thermal analysis

5.1. Thermal analysis of L₂

Thermal analysis of L₂ was investigated by TG/DTG.

The resulting curve was obtained under an open atmosphere in the range of 0–1000 °C with heating rate of 10 °C/min.

We have noticed that the decomposition of L₂ was in one step has started from ~ 200°C and has finished at ~ 400°C, and L₂ was almost pure. Most of L₂ was decomposed to high elements like CO₂, NO_x, SO₂, H₂O only 4% activated carbon was lifted, which confirmed the full thermolysis of this compound (see **Figure 20**).

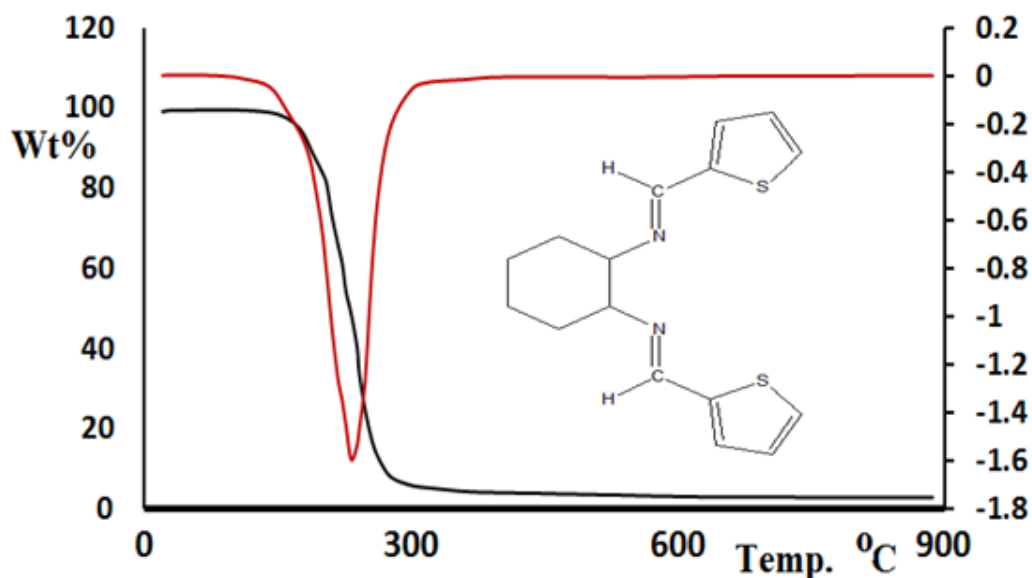


Figure 20: TG/DTG thermal curve of L₂

5.2. Thermal analysis of complex 4

The thermal stabilities of complex 4 was investigated by TG/DTG.

The curve was obtained at a heating rate of $10\text{ C}^\circ\text{ min}^{-1}$ in air atmosphere over the temperature range of $0 - 900\text{ C}^\circ$. The thermo-gravimetric analysis of this complex revealed the occurrence of the following steps.

- 1) Dehydration: loss of water molecules.
- 2) Ligand pyrolysis: ligand degradation.
- 3) Inorganic residue formation: Copper(II)bromide.
- 4) Removal bromide ions and Copper(II) oxide formation.

The TG/DTG spectra of complex 4 are mainly illustrating the expected steps of weight loss. The first step was losing of coordinated water molecule at $\sim 150\text{ C}^\circ$, as we have seen in IR spectra of complex 4. The sharp peaks in the range of 3140 to 3250 cm^{-1} was the evidence that water molecule was coordinated to copper center, and the losing percent of water was 2.5 %. The second decomposition step included L_2 degradation at temperature range of $200 - 300\text{ C}^\circ$ in the percent almost 65%. The third step included inorganic residue decomposition at temperature range of $450 - 600\text{ C}^\circ$ in a percent of 22 % which leads to the removal of bromide ions of CuBr_2 to form copper(II)oxide final product in the percent of 11%.

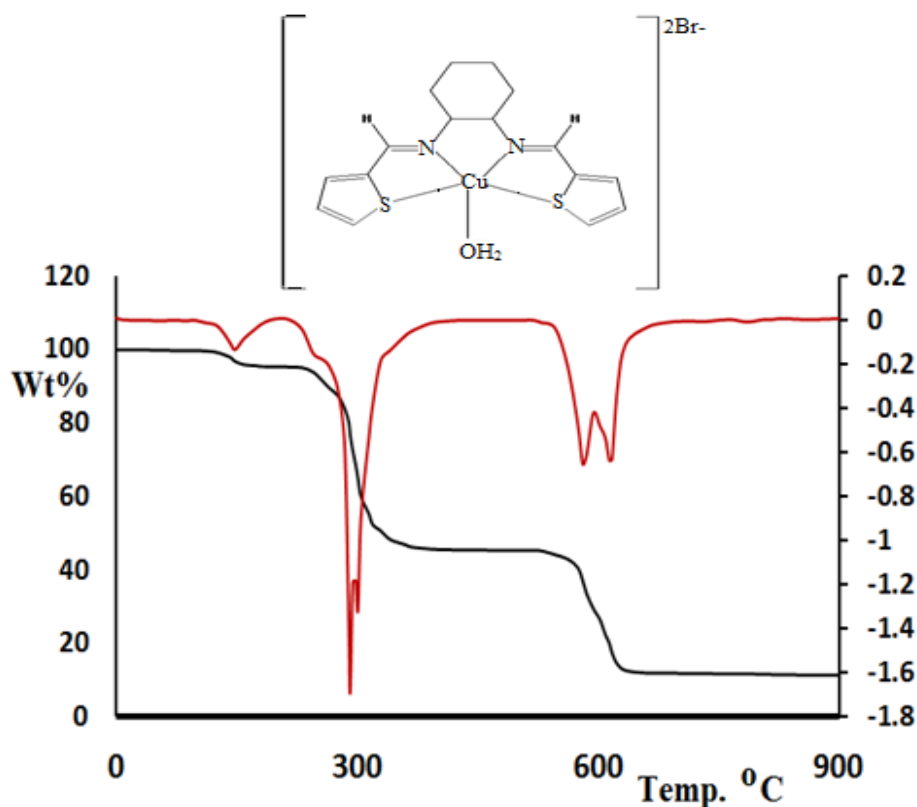


Figure 21: TG/DTG thermal curve of complex 4

6. Conclusion

New tetradentate Schiff base have been synthesized directly by mixing of thiophene-2-carbaldehyde and Cyclohexane-1,2-diamine through the condensation reaction and the product was N,N-bis-thiophen-2-ylmethylenecyclohexane-1,2-diamine, which was motioned with the symbol L_2 , and it was expected to be excellent tetradentate ligand.

It has been characterized by IR-spectroscopy, 1H , ^{13}C -NMR spectroscopy, TG/DTG.

It was reacted with CuX_2 (where $X = Br, Cl, OAc.$) in ethanol as solvent to form complex 4-6 (see **Charts 16-18**)

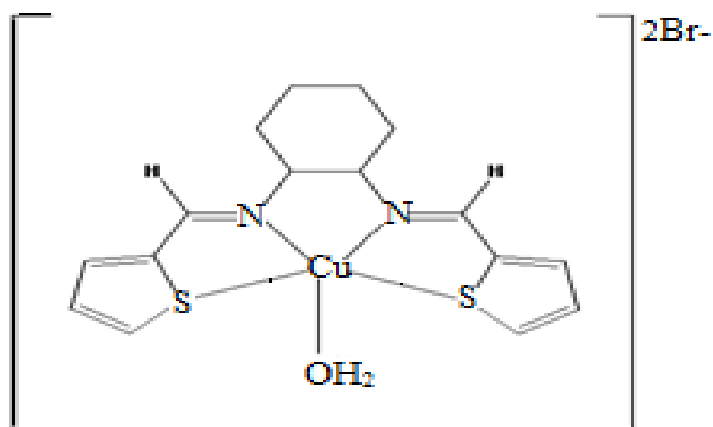


Chart 16: Expected structure of complex 4

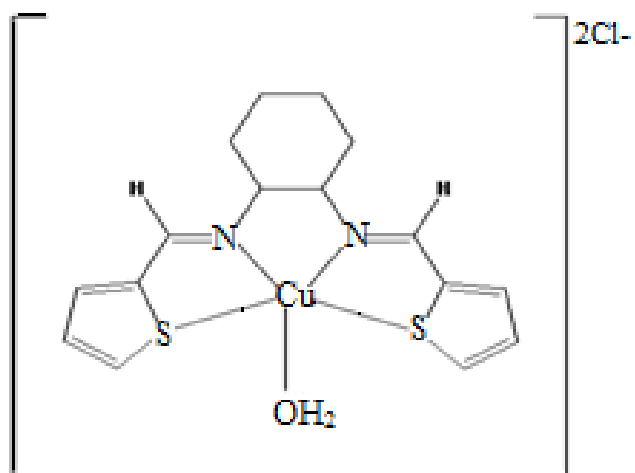


Chart 17: Expected structure of complex 5.

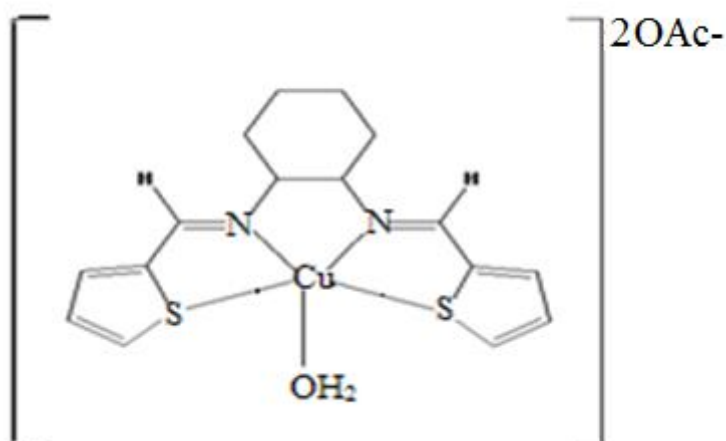


Chart 18: Expected structure of complex 6.

All complexes have been characterized by IR- spectroscopy, cyclic voltametry of complex **5**, and TG/DTG for complex **4**.

Suggestions

Through my studies of such compounds that have been synthesized and characterized in thesis, I suggested the following:

- ❖ To study the biological activities of **L₁**, **L₂** and their complexes **1-6**.
- ❖ To study the ability of the complexes **1-6** to bind with DNA of cancer cells.
- ❖ To synthesize the complexes **1-6** in crystalline form and solving them by XRD to confirm the exact isomer.
- ❖ To synthesis the same ligands **L₁**, **L₂** using more substituted starting materials.
- ❖ To experimenting another ways to synthesis the ligands **L₁**, **L₂** and complexes **1-6** in excellent yield
- ❖ To use another solvent in their synthesis.

References

1. Hussien, Z.; Yousef, E.; Ahmed, A.; Altaie, A. **Org. Med. Chem. Lett.**,2014,4,1.
2. Eissa, H.H.; **Org. Chem. Curr. Res.**,2013,3, 2.
3. Qin, W.; Long, S.; Panunzio, M.; Biondi, S. **Molecules**,2013,18,12264.
4. Saghatforoush, L.; Aminkhani, A.; Ershad, S.; Karimnezhad, G.; Ghammamy, S.; Kabiri, R. **Molecules**,2008, 13, 804.
5. Yang, Z.; Sun, P. **Molbank**,2006, M514, 1.
6. AL Zoubi, W. *Int. J. OrgChem.*,2013, 3, 73.
7. Osowole, A. A. **E-Jour. Chem.**,2008, 5, 130.
8. Sadeek, S.A.; Rafat, M. S.; Teleb, S. M. **Bull. Chem.Soc. Ethio.**, 2004, 18, 149.
9. Zemedede, Y.; S. A. **int. Jour. ChemTech Res.**,2014-2015, 7, 279
10. Pillai, M.R.A; Barnes, C.L.; Troutner, D.E.; *Schleper E.O. J. Crystal. Spec. Res.*, 1993, 23, 949
11. Kelode, R.S.; Mandlik. R.P. **J. Chem. Pharm. Res.**, 2012, 4, 418.
12. Khedr, A.; Marwani, H. **Int. J. ElectroChem. Sci.**, 2012, 7, 10074.
13. Bencini, A.; Lippolis, V., **Chem. Rev.**, 2010, 254, 2096
14. Ayad, M.; El-Boraey, H. *int. J. ChemTech Res.*,2014, 6, 266.
15. Gomathi, R.; Ramu, A. **Int. J. I. Res. Sci. Eng. Tech.**,2013, 2, 4853.
16. 16.Kadhim, Z. **J. Mater Environ. Sci.**,2015, 6, 693.
17. Zare, A.; Ata eineni, P. **life Sci. J.**,2012, 9, 2396.
18. Ibrahim, W.; Shamsuddin, M. **Crystal structure theory App.**, 2012, 1, 2.

19. Suzuki, T.; Kubota, T.; Kobayashi, J.; Eudistomidins H-K. **Med. Chem. Lett.** 2011, *21*, 4220.
20. Guggisberg, A.; Drandarov, K.; Hesse, M.; Protoverbine H. **Helv. Chim. Acta**, 2000, *83*, 3035.
21. Evans, R. F. **Aust. J. Chem.**, 1967, *20*, 1643.
22. Finch, H.; Peterson, E. A.; Ballard, S. A. **J. Am. Chem. Soc.**, 1952, *74*, 2016.
23. Russowski, D.; Canto, R.; Sanches, S.; D'Oca, M.; Fatima, A.; Carvalho, J. **Bioorg. Chem.**, 2006, *34*, 173.
24. Drandarov, K.; Guggisberg, A.; Hesse, M. **Helv. Chim. Acta**, 1999, *82*, 229.
25. Renson, B.; Merlin, P.; Dalozze, D.; Braekman, J.; Roisin, Y.; Pasteels, J. **Can. J. Chem.**, 1994, *72*, 105.
26. Bisceglia, J.; Garcia, M.; Massa, R.; Magri, M.; Zani, M.; Gutkind, G.; Orelli, L. **J. Heterocycl. Chem.**, 2004, *41*, 85.
27. Tu, S.; Miao, C.; Fang, F.; Youjian, F.; Li, T.; Zhuang, Q.; Zhang, X.; Zhu, S.; Shi, D. **Bioorg. Med. Chem. Lett.**, 2004, *14*, 1533.
28. Carvalho, G.; Dias, R.; Pavan, F.; Leite, C.; Silva, V.; Diniz, C.; de Paula, D.; Coimbra, E.; Retailleau, P.; da Silva, A. **Med. Chem.**, 2013, *9*, 351.
29. Agbaje, O.; Fadeyi, O.; Fadeyi, S.; Myles, L.; Okoro, C. **Bioorg. Med. Chem. Lett.** 2011, *21*, 989.
30. Hwang, J.; Kim, H.; Jo, S.; Park, E.; Choi, J.; Kong, S.; Park, D.; Heo, J.; Lee, J.; Ko, Y.; Choi, I.; Cechetto, J.; Kim, J.; Lee, J.; No, Z.; Windisch, M. **Eur. J. Med. Chem.** 2013, *70*, 315.

31. Martirosyan, A.; Tamazyan, R.; Gasparyan, S.; Alexanyan, M.; Panosyan, H.; Martirosyan, V.; Schinazi, R. **Tetrahedron Lett.**, 2010, *51*, 231.
32. Enders, D.; Wortmann, L. **Heterocycles**, 2002, *58*, 293.
33. Khan, M.; Gupta, M. **Pharmazie**, 2002, *57*, 377.
34. Billman, J.; Khan, S. **J. Med. Chem.**, 1966, *9*, 347.
35. Billman, J.; Khan, S. **J. Med. Chem.**, 1965, *8*, 498.19.
36. Azam, M.; Warad, I.; Al-Resayes, S.; Alzaqri, N.; Khan, M.; Pallepogu, R.; Dwivedi, S.; Musarrat, J.; Shakir, M. **J. Molec. Strut.**, 2013, *104*, 48.
37. Azam, M.; Warad, I.; Al-Resayes, S.; Zahin, M.; Ahmad, I.; Shakir M. **Z. Anorg. Allg. Chem.**, 2012, *638*, 881.
38. Schmidt, M; Wiedemann, D.; Grohmann, A. **Inorg. Chim. Acta**, 2011, *374*, 514.
39. He, X.-F.; Vogels, C. M.; Decken, A.; Westcott, S. A. **Polyhedron**, 2014, *23*, 155.
40. Massacesi M., Pinna R., Biddau M., Ponticelli G., Zakharova I. A., **Inorg. Chem. Acta**, 1983, *80*, 151.
41. Yalcin, I.; Oren, I.; Sener, E.; Akin, A.; Ucarturk, N. **Eur. J. Med. Chem.**, 1992, *27*, 401.
42. Schlangen, M.; Neugebauer, J.; Reiher, M.; Schröder, D.; Pitarch López, J.; Haryono, M.; Heinemann, F.W.; Grohmann, H. Schwarz, **J. Am. Chem. Soc.**, 2008, *130*, 4285.
43. Boyd, J.P.; Schlangen, M.; Grohmann, A. ; Schwarz, H. **Helv. Chim. Acta**, 2008, *91*, 1430.

44. Grohmann, A. **Dalton Trans.**, 2010, 39,1432.
45. Warad, I.; Alruwaili, A.; Al-Resayes, S.; Choudhary, M.I.; Yousuf, Y. **ActaCrystallogr. Sect. E: Struct. Rep. Online**, 2012, 68, o1786.
46. Haddad, S.F.; Warad, I.; Jodeh, S.; Ben Hadda, T. **ActaCrystallogr. Sect. E: Struct. Rep. Online**, 2013, 69, o569.
47. Abu-Obaid, A.; Asadi, A. I.; Alruwaili, A.; Atieh, H.; Khlaif, Sh.; Ben Hadda, T.; Radi, S.; Hammouti, B.; Warad, I. **Molbank**, 2015, M838, 6.
48. Bruker, APEX2, SAINT and SADABS, Bruker AXS Inc., Madison, Wisconsin, UA, 2009.
49. Sheldrick, G. M. **ActaCryst.**, 2008, A64, 112.
50. Spek, A. L. **ActaCryst.**,1990, A46, 34.
51. Macrae, C. F., Bruno, I. J.; Chisholm, J. A.; Edgington, P. R.; McCabe, P.; Pidcock, E.; Rodriguez-Monge, L.; Taylor, R.; Van de Streek, J.; Wood, P. A. **J. Appl. Cryst.**,2008, 41, 466.
52. Septioglu, E; Aytemir, MD; Calis, U, **PubMed**, 2005, 5, 64.
53. Gunasekaran, S.; Balaji, R.A.; Kumaresan, S.; Anand, G.; Srinivasan, S.; **Can. J. Anal.Sci. Spectrosc.**,2008, 53, 149.
54. Karpagam, J.; Sundaraganesan, N.; Sebastain, S.; Manoharan, S.; Kurt, M.J. **Raman Spectrosc.**, 2010, 41, 53.
55. Cremer, D.; Pople, J. A., **J. Amer. Chem. Soc.**, 1975, 97, 1354.
56. Spackman, M. A.; McKinnon, J. J.; Jayatilaka, D. **CrystEngComm**,2008, 10, 377.

57. Wolff, S. K.; Grimwood, D. J.; McKinnon, J. J.; Jayatilaka, D.; Spackman, M. A. **CrystalExplorer 3.0, University of Western Australia, Perth, Australia, 2001.**
58. Spackman, M. A.; McKinnon, J. J.; Jayatilaka, D. **CrystEngComm., 2008, 10, 377.**

جامعة النجاح الوطنية
كلية الدراسات العليا

تحضير و تشخيص و قياس درجة ترابط الحمض النووي
الاميني بعمققات النحاس/المرتبطة بقواعد شيف
(SNNS) الرباعية

إعداد

ابتهاال نضال محمود عودة

إشراف

أ.د. إسماعيل وراة

أ.د. محمد النوري

قأمت هذه الأطروحة استكمالاً لمتطلبات الحصول على درجة الماجستير في الكيمياء بكلية
الدراسات العليا في جامعة النجاح الوطنية في نابلس، فلسطين

2016

ب

تحضير و تشخيص و قياس درجة ترابط الحمض النووي الاميني بعمققات النحاس/المرتبطة

بقواعد شيف(SNNS) الرباعية

إعداد

ابتهال نضال محمود عودة

إشراف

أ.د. إسماعيل وراذ

أ.د. محمد النوري

الملخص

في هذه الدراسة تم تحضير نوعين من المركبات العضوية المحتوية على ذرات مانحة للالكترونات هما النيتروجين والكبريت, حيث عملت هذه المركبات كمتصلات عديدة المنح في حالة مفاعلها مع أيونات النحاس الثنائية.

في الجزء الأول من الدراسة, تم تحضير L_1 الحلقي من خلال مفاعلة 5-

bromothiophene-2-carbaldehyde, 2,2-dimethyl-1,3-

propanediamine حيث أثبتت أفضلية الإغلاق على تكوين قواعد شيف.

جاءت نتائج قياس حيود الطيف السيني لتؤكد تكوّن L_1 حيث تم التعرف على الصيغة البنائية لمثل هذا المركب.

بمفاعلة L_1 مع أملاح النحاس CuX_2 , $X = Br, Cl, OAc$ في وسط كحولي تم عزل

ثلاثة معقدات بالصيغة $[Cu(L_1)_2X]X$ وهي معقدات أحادية الأيون.

في الجزء الثاني, تم تحضير قاعدة شيف L_2 من النوع N_2S_2 من خلال تفاعل التكثيف

لكل من

thiophene-2- carbaldehyde, cyclohexane-1.2-diamine في وسط

كحولي.

ج

قيمت قدرة هذا المتصل رباعي المنح على الترابط مع أيونات النحاس الثنائية من خلال مفاعلتها مع CuX_2 حيث عزلت هذه المعقدات لتظهر بالصيغة $[CuL_2H_2O]2X$ وهي صيغة المعقد ثنائي الأيون وقد تم التحقق من صيغتها البنائية بواسطة العديد من القياسات الطيفية والحرارية.